





3 | Applied and Industrial Microbiology | Research Article

# Overexpression of native carbonic anhydrases increases carbon conversion efficiency in the methanotrophic biocatalyst *Methylococcus capsulatus* Bath

Spencer A. Lee, <sup>1</sup> Jessica M. Henard, <sup>1</sup> Robyn A. C. Alba, <sup>1</sup> Chance A. Benedict, <sup>1</sup> Tyler A. Mayes, <sup>1</sup> Calvin A. Henard

**AUTHOR AFFILIATION** See affiliation list on p. 18.

ABSTRACT Methanotrophic bacteria play a vital role in the biogeochemical carbon cycle due to their unique ability to use CH<sub>4</sub> as a carbon and energy source. Evidence suggests that some methanotrophs, including Methylococcus capsulatus, can also use CO<sub>2</sub> as a carbon source, making these bacteria promising candidates for developing biotechnologies targeting greenhouse gas capture and mitigation. However, a deeper understanding of the dual CH<sub>4</sub> and CO<sub>2</sub> metabolism is needed to guide methanotroph strain improvements and realize their industrial utility. In this study, we show that M. capsulatus expresses five carbonic anhydrase (CA) isoforms, one α-CA, one γ-CA, and three β-CAs, that play a role in its inorganic carbon metabolism and CO<sub>2</sub>-dependent growth. The CA isoforms are differentially expressed, and transcription of all isoform genes is induced in response to CO2 limitation. CA null mutant strains exhibited markedly impaired growth compared to an isogenic wild-type control, suggesting that the CA isoforms have independent, non-redundant roles in M. capsulatus metabolism and physiology. Overexpression of some, but not all, CA isoforms improved bacterial growth kinetics and decreased CO<sub>2</sub> evolution from CH<sub>4</sub>-consuming cultures. Notably, we developed an engineered methanotrophic biocatalyst overexpressing the native α-CA and  $\beta$ -CA with a 2.5-fold improvement in the conversion of CH<sub>4</sub> to biomass. Given that product yield is a significant cost driver of methanotroph-based bioprocesses, the engineered strain developed here could improve the economics of CH<sub>4</sub> biocatalysis, including the production of single-cell protein from natural gas or anaerobic digestionderived biogas.

**IMPORTANCE** Methanotrophs transform  $CH_4$  into  $CO_2$  and multi-carbon compounds, so they play a critical role in the global carbon cycle and are of interest for biotechnology applications. Some methanotrophs, including *Methylococcus capsulatus*, can also use  $CO_2$  as a carbon source, but this dual one-carbon metabolism is incompletely understood. In this study, we show that *M. capsulatus* carbonic anhydrases are critical for this bacterium to optimally utilize  $CO_2$ . We developed an engineered strain with improved  $CO_2$  utilization capacity that increased the overall carbon conversion to cell biomass. The improvements to methanotroph-based product yields observed here are expected to reduce costs associated with  $CH_4$  conversion bioprocesses.

**KEYWORDS** methanotroph, carbonic anhydrase, C1 metabolism, methane, carbon dioxide, greenhouse gas

M ethanotrophic bacteria (methanotrophs) use methane (CH<sub>4</sub>) as both a carbon and energy source. These unique microbes are ubiquitous in terrestrial and aquatic ecosystems where they play a vital role in the biogeochemical cycling of CH<sub>4</sub>, a potent greenhouse gas (GHG). Due to their unique metabolism, methanotrophs are

**Editor** Susannah Green Tringe, E. O. Lawrence Berkeley National Laboratory, Berkeley, California, USA

Address correspondence to Calvin A. Henard, Calvin.Henard@unt.edu.

Some aspects of this work are included as part of a U.S. patent application (PCT/US2024/034678).

See the funding table on p. 18.

Received 10 June 2024 Accepted 23 July 2024 Published 27 August 2024

Copyright © 2024 Lee et al. This is an open-access article distributed under the terms of the Creative Commons Attribution 4.0 International license.

used industrially for the conversion of  $CH_4$ -rich gas to valuable products, including single-cell protein and polyhydroxyalkanoates (1, 2). Furthermore, methanotrophs may be leveraged for direct air capture of  $CH_4$  for GHG mitigation and combating climate change (3, 4).

In these bacteria, CH<sub>4</sub> assimilation is mediated by cytoplasmic- or membrane-associated CH<sub>4</sub> monooxygenases (MMO), which use molecular oxygen to oxidize CH<sub>4</sub> to methanol (CH<sub>3</sub>OH) (5, 6). CH<sub>3</sub>OH is further oxidized to formaldehyde (CH<sub>2</sub>O) in the periplasm by calcium- or lanthanide-dependent CH<sub>3</sub>OH dehydrogenases. The CH<sub>2</sub>O can enter central metabolism in the cytosol by (i) directly condensing with a C<sub>5</sub> sugar in the ribulose monophosphate (RuMP) cycle, (ii) conversion to methylene tetrahydrofolate (H<sub>4</sub>F) via methylene tetrahydromethanopterin- and H<sub>4</sub>F-C<sub>1</sub> transfer pathways followed by condensation with glycine in the serine cycle, or (iii) complete oxidation to carbon dioxide (CO<sub>2</sub>), which can be assimilated via autotrophic pathways (7). Methanotrophs are broadly categorized based on their preferred route of CH2O metabolism, wherein Gammaproteobacterial methanotrophs use the RuMP cycle, Alphaproteobacterial methanotrophs use the serine cycle, and Verrucomicrobia/Candidate phylum NC10 methanotrophs use the ribulose-1,5-bisphophate carboxylase/oxygenase (RubisCO) and the Calvin cycle to reassimilate CH<sub>4</sub>-derived CO<sub>2</sub> (8). Notably, all aerobic methanotrophs completely oxidize a percentage (Gammaproteobacteria and Alphaprotebacteria) or all (Verrucomicrobia/Candidate phyla NC10) of assimilated CH<sub>4</sub> to CO<sub>2</sub> (9–11).

Methylococcus capsulatus str. Bath is a model methanotroph that has served to elucidate several fundamental aspects of methanotrophy (12), including structural elucidation of the particulate MMO (6, 13, 14), and characterization of the generalizable "copper switch" physiological response to copper starvation in methanotrophs that encode both the soluble and particulate MMO forms (15, 16), among others. M. capsulatus belongs to a phylogenetical distinct lineage of methanotrophs within the Methylococcaceae family of Gammaproteobacterial methanotrophs (Type Ib) that includes the Methylocaldum, Methylococcus, Methylogaea, Methylomagnum, and Methyloterricola genera (17). These methanotrophs encode RubisCO, but, in contrast to Verrucomicrobia, M. capsulatus derives its biomass from CH<sub>4</sub>-derived formaldehyde via the RuMP cycle and CO<sub>2</sub> via RubisCO (18). Previous studies show that M. capsulatus RubisCO is expressed and active (19–21) and that both the enzyme and CO<sub>2</sub> are essential for bacterial cultivation (18).

Most RubisCO enzymes exhibit poor efficiency with low catalytic rate constants and substrate specificity (22). Thus, many autotrophic bacteria have developed inorganic carbon concentrating mechanisms (CCMs) to improve CO<sub>2</sub> assimilation (23). One of the most characterized CCMs are carboxysomes in photoautotrophic cyanobacteria, which are proteinaceous "organelles" that house RubisCO, a bicarbonate transporter, and carbonic anhydrase (24). Genes encoding the carboxysome structural shell proteins are not found in the *M. capsulatus* genome and carboxysomes are not visualized in electron micrographs, providing strong evidence that *M. capsulatus* does not encode these structures to enhance CO<sub>2</sub> assimilation. CCMs in non-phototrophic autotrophic bacteria without carboxysomes are not well understood. *M. capsulatus* is cultivated aerobically and relatively low concentrations of CO<sub>2</sub> in a CH<sub>4</sub>-rich gas mixture permit growth (18), so this methanotroph may possess alternative CCMs to enhance RubisCO CO<sub>2</sub> substrate specificity.

CAs are metalloenzymes that mediate the reversible hydration of  $CO_2$  to  $H^+$  and bicarbonate (HCO $_3$ ) and are represented in all domains of life (25). These enzymes typically have a substrate preference for either  $CO_2$  or  $HCO_3^-$ , which can promote  $CO_2$  conversion or production depending on the environmental condition (25). Bacteria typically encode one or more of the  $\alpha^-$ ,  $\beta^-$ , and/or  $\gamma$ -classes of CAs, which contribute to their survival and adaptation in diverse environments through their roles in pH homeostasis, metabolic pathway regulation, ion transport, and  $CO_2$  fixation and conversion (25–27). In many autotrophic bacteria, CAs mediate a CCM by sequestering  $CO_2$  and converting it to  $HCO_3^-$ , which does not readily diffuse from the cell (28). In turn,

Month XXXX Volume 0 Issue 0 10.1128/msphere.00496-24 **2** 

intracellular CAs convert  $HCO_3^-$  to  $CO_2$  colocalized with RubisCO, increasing substrate availability and conversion efficiency (29, 30). CAs have been successfully utilized to enhance carbon capture and growth of engineered microbes (31–36), underscoring their biotechnology potential to sequester atmospheric  $CO_2$  and mitigate GHGs.

In this study, we used a genetics approach to evaluate the role(s) of five annotated CAs in *M. capsulatus* metabolism. We show that the five distinct CA isoforms are transcribed and exhibit differential induction in response to CO<sub>2</sub> availability. Experiments evaluating the pharmacological inhibition of *M. capsulatus* CAs and the growth of strains deficient in individual CAs provide evidence that these enzymes play critically important, non-redundant roles in *M. capsulatus* metabolism and physiology. Overexpression of CAs improved *M. capsulatus* growth kinetics and CH<sub>4</sub> conversion efficiencies. Our results advance the understanding of inorganic carbon metabolism in methanotrophic bacteria and highlight a genetic engineering strategy that leverages CAs to mitigate both CH<sub>4</sub> and CO<sub>2</sub> GHGs.

### **MATERIALS AND METHODS**

# **Bacterial cultivation**

Bacterial strains used in this study are shown in Table 1. M. capsulatus Bath cultures were routinely maintained with nitrate mineral salts (NMS) solid medium in stainless steel gas chambers supplied with 20% CH<sub>4</sub> in the gas phase as previously described (37). Strains were grown in 150 mL vials containing 10 mL of liquid NMS medium or 250 mL vials containing 20 mL of liquid NMS medium. After inoculation with plate-derived biomass or diluted seed culture, vials were crimped with gray butyl stoppers to create gas-tight seals. CH<sub>4</sub> was added to the headspace to reach a final CH<sub>4</sub> concentration of 20% in the air (vol/vol), and cultures were incubated at 37°C at 200 rpm orbital shaking. Continuous gas cultivation was performed using a custom mid-throughput gas fermentation reactor fitted with 150 mL, 38 mm Kimax cultivation tubes supplied with mixed gas via rotameters and stainless steel sparge stones. 100 mL cultures were inoculated with plate-derived biomass to  $OD_{600} = 0.1$  and supplied with 20%  $CH_4/2\%$   $CO_2$  in air (vol/vol) at a flow rate of 1 vol gas/volume culture/min (vvm) premixed with gas-specific mass flow controllers. Culture samples ( $\sim 100~\mu L$ ) were periodically extracted from vials with a syringe to measure bacterial growth via dilution plating or spectrophotometrically at OD<sub>600</sub> using a Nanodrop spectrophotometer. High-resolution bacterial growth was measured every 20 seconds by Cell Growth Quantifier (CGQ) optical sensors (Scientific Bioprocessing) to determine growth rates. The backscatter arbitrary units measured by the CGQ sensors were transformed to OD<sub>600</sub> using linear regression of measured initial and final  $OD_{600}$  measurements. The CGQ sensor limit of detection is equivalent to  $OD_{600}$ 0.5.

# Carbonic anhydrase knockout and overexpression strain construction

Primers used for cloning and genetic manipulations are shown in Table 2. All PCRs were performed with Q5 High-Fidelity 2X Master Mix following the manufacturer's recommendations (New England Biolabs), and PCR annealing temperatures were determined using the NEB Tm Calculator tool. Plasmids were assembled using NEBuilder HiFi DNA Assembly Master Mix following the manufacturer's vector:insert molar ratio recommendations, but total reaction volumes were minimized and typically between 4 and 10 μL, depending on the amount of assembled fragments (New England Biolabs). *M. capsulatus* Bath carbonic anhydrase (MCA0910, MCA1080, MCA1422, MCA1665, and MCA2797) knock-out strains were created by amplifying 1,000 bp DNA regions upstream and downstream flanking the genes of interest from genomic DNA and an Flp recombinase recognition target (FRT)-flanked gentamicin or kanamycin resistance cassette from pPS856 or pKD13, respectively. The 1 kb upstream-antibiotic resistance-1kb downstream was assembled with pK18mobpheS linearized *via* PCR using primers oCAH576/577 and

TABLE 1 Strains and plasmids

Strains			
Name	Genotype	Source	
Methylococcus capsulatus str. Bath	Wild type	Lab Stock	
ΔCA1::Kn <sup>R</sup>	MCA0910 gene replaced with an FRT-flanked Gm <sup>R</sup> cassette	This study	
ΔCA2::Gm <sup>R</sup>	MCA1080 gene replaced with an FRT-flanked Kn <sup>R</sup> cassette	This study	
ΔCA3::Gm <sup>R</sup>	MCA1422 gene replaced with an FRT-flanked Gm <sup>R</sup> cassette	This study	
$\Delta CA4::Kn^R$	MCA1665 gene replaced with an FRT-flanked Kn <sup>R</sup> cassette	This study	
ΔCA5::Gm <sup>R</sup>	MCA2797 gene replaced with an FRT-flanked Gm <sup>R</sup> cassette	This study	
pCA1 Bath	M. capsulatus with inducible overexpression of MCA0910	This study	
pCA2 Bath	M. capsulatus with inducible overexpression of MCA1080	This study	
pCA3 Bath	M. capsulatus with inducible overexpression of MCA1422	This study	
pCA4 Bath	M. capsulatus with inducible overexpression of MCA1665	This study	
pCA5 Bath	M. capsulatus with inducible overexpression of MCA2797	This study	
pCA2/3 Bath	M. capsulatus with inducible overexpression of MCA1080 and MCA1422	This study	
pCA1 Δ <i>CA1::Gm<sup>R</sup></i>	<i>M. capsulatus</i> $\Delta$ <i>CA1::Gm</i> <sup>R</sup> with inducible overexpression of MCA0910	This study	
pCA3 Δ <i>CA3::Gm</i> <sup>R</sup>	M. capsulatus∆CA3::Gm <sup>R</sup> with inducible overexpression of MCA1422	This study	
pCA5 Δ <i>CA5::Gm<sup>R</sup></i>	M. capsulatus∆CA5::Gm <sup>R</sup> with inducible overexpression of MCA2797	This study	
Escherichia coli str. Zymo 10B	F- mcrA Δ(mrr-hsdRMS-mcrBC) Φ80lacZΔM15 ΔlacX74 recA1 endA1	Zymo Research	
	araD139 Δ(ara leu) 7697 galU galK rpsL nupG		
E. coli \$17-1	Tp' Sm' recA thi pro hsd(r m <sup>+</sup> )RP4-2-Tc::Mu::Km Tn7	ATCC 47055	
Plasmids			
Name	Description	Source	
pCAH01	P <sub>tetA</sub> bla tetR CoE1ori F1 oriV oriT trfA ahp	(38)	
pCA1	pCAH01 plasmid with M. capsulatus CA1 (MCA0910)	This study	
pCA2	pCAH01 plasmid with M. capsulatus CA2 (MCA1080)	This study	
pCA3	pCAH01 plasmid with M. capsulatus CA3 (MCA1422)	This study	
pCA4	pCAH01 plasmid with M. capsulatus CA4 (MCA1665)	This study	
pCA5	pCAH01 plasmid with M. capsulatus CA5 (MCA2797)	This study	
pCA2/3	pCAH01 plasmid with <i>M. capsulatus</i> CA2 (MCA1080) and CA3 (MCA1422) in an operon.	This study	
pK18mobsacB	Marker-exchange mutagenesis suicide plasmid with <i>sacB</i> (39) counterselectable marker		
pK18mobpheS	Marker-exchange mutagenesis suicide plasmid with <i>pheS</i> This study counterselectable marker		
pPS856	Source of FRT-flanked aacC Gm <sup>R</sup> cassette	(40)	
pKD13	Source of FRT-flanked <i>aph</i> Kn <sup>R</sup> cassette (41)		

transformed into chemically competent E. coli DH10b. Sequence-confirmed plasmids were then transferred into S17-1 E. coli via chemical transformation to mediate biparental conjugation with M. capsulatus as previously described (42). M. capsulatus transformants were selected on NMS containing 50 µg/mL kanamycin or 20 µg/mL gentamicin and 10 mM 4-chloro-phenylalanine to select for double-crossover events. Antibioticand 4-chloro-phenyalanine-resistant transformant colonies were screened by PCR to confirm the replacement of a CA locus with the antibiotic resistance cassette. Notably, antibiotic resistant, small, atypical CA KO transformant colonies typically appeared 4 weeks [compared to 1 week for wild type (WT)] after plating on a selective medium. The pK18mobpheS plasmid was generated following methods found in Ishikawa et al. (43). Here, a M. capsulatus-mutated pheS gene (minimally codon-optimized to enable synthesis) encoding the  $\alpha$ -subunit of phenylalanyl-tRNA synthetase containing two missense mutations (A306G and T252A) was synthesized as a gblock by Integrated DNA Technologies and assembled with pK18mobsacB linearized with primers oCAH572/ oCAH573 to replace sacB with the mutated pheS gene.

Downloaded from https://journals.asm.org/journal/msphere on 28 August 2024 by 47.38.247.126.

Research Article mSphere

**TABLE 2** Synthetic DNA and primers<sup>a</sup>

	Fragment/Primer name	Sequence	Purpose
GTGGCAGAATTAGACCAGGTACGCGTCCGCTATCTGGGGAA  GAAGGGCGAGTTCACCGAGCAGAGAAGACGCTGGGCACG  CTCTCGCCGGAAGAACGCAAGGAATTTGGTCAGCGCGTCAA  TCAGGCACCGTGAACGCAGCTCCTGGAGCGCGCCG  AAGGCGCCGCTGGAAGCCCTGGAAGCCGCGGCTGA  GTAGCGAGACGATGCAGCGCTCCTGGAGCGCGCTGA  GTAGCGAGACGATCGAAGCCCTCGGCACCGCGGCTGA  GTAGCGAGACGATCGATGTCACGCTCCCTGGCACGCGGCTGA  CGACTGGGAGGACTGCTCCGGTCACGTTAACCCTCCGACG  CATCACCAAGGCTGTTCCGGTCACGTTAACCCTCCGACG  CATCACCAAGGCTGTTCCGGTCACTTAGACCTTCCAAGCCT  TGAATATTCCCGCCCACCATCCGGCGCGCGCGATGCATGAC  ACATTCTACTTCTCCGAACATCTCCTCCTGCGTACCCACCC	M. capsulatus codon-optimized pheS	gtacataaaaaaggagacatgaacgATGAACTCGTCGCCCGAATCCAC	gblock used to generate pK18mob-
GAAGGCGAGTTCACCGAGCAGATGAAGACCCTTGGCACG CTCTCGCCGGAAGAACCCAAGGAATTTGGTCAGCGCGTCAA TCAGGCACGTGACGAGACCCGAAGCCCTGGAGCGCCGC AAGGCGCGCTGCAAGCCCGAAGCCCGACGCGCGCTGA GTAGCGAGACGCGATCGATGTCACGCTCCCTGGAGCGCAG CGACTGGGAGGATCGATGTCACGCTCCCTGGCCGTGGGCAG CGACTGGGAGGATCGATGTCACGCTCCCTGTACCCTCCGACG CATCACCAGGCTGTTCCGGTCACTTTGCTTCAGCGTCGTGG AAGGCCCGGAGATTGAAGACGACCTTTCATAACTTCGAAGCCT TGAATATTCCCGCCCCACCATCCGGCGCGCGCGCGATGCATGAC ACATTCTACTTCTCCGAACATCTCCTCCTGCGTACCCACACC AGCCCGGTCCACATCCGGCGTTATGGAGTCCCGACCACCC CGCTCCGGGTGATAGCCCCCCGGACGGGTTTTCATCAGTGCGA CAGCGACCTGACCCACACCGCGATGTTTCACCAGGTCGAG GCTTCTTGGGTTGATGAGCACGCGTATTTCACCAGGTCGAAG GCTTCTTGGGTTGATTAGACAGGTTCCTTCGCCGATCTTGAAG GGCACGTTGATTAGAGTTCCTTACCGGCTTCTTCGAGAAGAC TGTGCCGTACGGTTCCGGCCGAGCTACTTCCCGGTTTGCAGG ACCCTCGGCCCAGGGTCCACACCGCCGATCTTCCGCGTACCAGGC CCGTGGCCAGGGTCCACACCGCCGATCTTCCCGGTTCGAGA GGCACGTTGTATGAGTTCCATCCAGGTCCGTCTCGAGA GCCTGGGCCTGACCAGCAGCTACTTCCGGCTTCTGAGG GCCTGGGCATCGACCCCGAACGATTCAGCCTGCCTGCAGG CCCTGGGCCTGACCCCGAACGATTCAGCCTCTCCCGGCTTCGAGG CCCTGGGCCTGCCCGGCTCTCCCAGGCTCTTCCAGG CCCTGGGCATCGACCCCGAACGGTATTCAGGCTGCTTCCGAGG CCCTGGGCATCGACCCCGAACGGTATTCAGGCTTCCCGCCTTCC GGCCTGGGCATCGACCCCGAACGGTATTCCGGCCTTCCCGGC CCGGGCATCGACCCCGAACGGTATTCCGGCCTTCCCGCCTTCCCGGC CCTGGGCATCGACCCCGAACGGTATTCCGGCCTTCCCGCCTTCCCGGC CCGCCCAGGCCTCGACCCCGAACGGTATTCCGGCCTTCCCCGCCTTCCCGCCTTCCCGCCTTCCCGCCTTCCCGCCTTCCCCGCCTTCCCCGCCTTCCCCGCCTTCCCCGCCTTCCCCGCCTTCCCCTTCCCCCC	T252A /A306G	CCTGGAGCAGGCAGGCTGCTGGCCGCCGCGGGAAGC	pheS marker exchange mutagenesis
CTCTCGCCGGAAGAACGCAAGGAATTTGGTCAGCGCGTCAA TCAGGCACGTGACGAGTTCCAGCGGCTCCTGGAGCGCCGC AAGGCGGCGCTGGAAGCCGAAGCCCTGGCAGGCGCGCGC AAGGCGGGCGCTGGAAGCCGAAGCCCTGGCCGGCGGCTGA GTAGCGAGACGATCGATGCACCCGGTCACGTTAACCCTCCCGACG CGACTGGGAGACTGCACCCGGTCACGTTAACCCTCCCGACG CATCACCAGGCTGTTCCGGTCAGTTGGCTTCAGCGTCGTGG AAGGCCCGGAGATTGAAAGACGACTTTCATACTTCGAAGCCT TGAATATTCCCCGCCCACCATCCGGCGCGCGCGCGCATGCAT		GTGGCAGAATTAGACCAGGTACGCGTCCGCTATCTGGGGAA	plasmid
TCAGGCACGTGACGAGTTCCAGCGGCTCCTGGAGCGCCGC AAGGCGGCGCTGGAAGCCCGAAGCCCTGGCACGGCGGCTGA GTAGCGAGGACGATCGATGTCACGCTCCCTGGCCGTGGGCAG CGACTGGAGGACGACCCCCGTCACGTTAACCCTCCGACG CATCACCAGGCTGTTCCGGTCACGTTCAGCTTCAGCGTCGTGG AAGGCCCGGAGATTGAAGCACCTTTCATAACTTCGAAGCCT TGAATATTCCCGCCCCCCACCATCCGGCGCGCGCGATGCATGAC ACATTCTACTTCTCCGAACATCTCCTCTGCGTACCCCACCC AGCCCGGTCCAGATCCGCGTCAGTATGGAGTCCGGCAGCCCC CGCTCCGGGTGATAGCCCCCGGCGCGCGCGCGCGCGCGCG		GAAGGGCGAGTTCACCGAGCAGATGAAGACGCTGGGCACG	
AAGGCGGCGCTGGAAGCCGAAGCCCTGGCACGGCGGCTGA GTAGCGAGACGATCGATGTCACGCTCCCTGGCCGTGGGCAG CGACTGGGAGGACTGCACCCGGTCACGTTAACCCTCCGACG CATCACCAGGCTGTTCCGGTCAGTTGGCTTCAGCGTCGTGG AAGGCCCGGAGATTGAAGACGACTTTCATAACTTCGAAGCCT TGAATATTCCCGCCCACCATCCGGCGCGCGCGCGATGCATGAC ACATTCTACTTCTCCGAACATCTCCTCCTGCGTACCCACACC AGCCCGGTCCAGATCCGCGTTATGGAGTCCGGCAGCCCC CGCTCCGGGTGATAGCCCCCGACAGCGGTCTATCGGTGCGA CAGCGACCTGACCCACACCCCGGACGGCTCTATCGGTGCGA CAGCGACCTGACCCACACCCCGATGTTCACCAGGTCGAG GCTTCTGGGTTGATGAGGTTCCTTACCGGCTTCTGAAG GGCACGTTGTATGAGTTCCTTACCGGCTTCTTCGAGAAGGAC TGTGCCGTACGGTCCGACTTCTTCCGGCTTCTTCGAGAAGGAC TGTGCCGTACCGGCTGCAATCCAGTCGTCTTCTCGCGATTG GTCGGGCCGAGGTTGCAAGCATTCAGGCTGCATG GTCGGGCCTGCCGGGTATGCAAGCATTCAGGCTGCAG GGTGATGGGCTGCCGAGTTCCAGCTTCTTCGAGG CCGTGGGCGTCGCCGAACGGTATTCAGGCTTCTCGAGG CCGTGGGCGTCGACCCCGAACGGTATTCGGGCTTCCGCCTTC GGCCTGGGCCTCGACCCCGAACGGTATTCGGGCTTCCGCCACGCA TCAACGACCTTCGCCGTCTCTTCTCGAGATGCTTCCCCGCTTCC TGCGCCAGTTCCAGCCCCTCTTCTTCGAGAATGCTTCCGCCTTCC TGCGCCAGTTCCAGCCCCTCTTCTTCGAGAATGCTTCCGCCTTCC TGCGCCAGTTCCAGCCCCTCTTCTTCGAGAATGCTTCCCCCTTCCC TGCGCCAGTTCAACCCCTTCTTCTTCGAGAATGCTTCGCCTTTCC TGCGCCAGTTCAACCCCTTCTTCTTCGAGAATGATCTGCCCTTCCC TGCGCCAGTTCAACCCCTTCTTCTTCGAGAATGATCTGCCCTTCC TGCGCCAGTTCAACCCCTTCTTCTTCGAGAATGATCTGCCCTTCC TGCGCCAGTTCAACCCCTTCTTCTTCAGAAATGATCTGCCGCTTCC TGCGCCAGTTCAACCCCTTCTTCTTCTCAAAAATGATCTGCCCTTCC TGCGCCAGTTCAACCCCTTCTTCTTCAAAAAATGATCTGCCCTTCC TGCGCCAGTTCAACCCCTTCTTCTTCTCAAAAATGATCTGCCCTTCC TGCGCCAGTTCAACCCCTTCTTCTTCTAAAAAATGATCTGCCCTTCC TGCGCCAGTTCAACCCCTTCTTCTTCTAAAAAATGATCTGCCCTTCC TGCGCCAGTTCAACCCCTTCTTCTTCTAAAAAATGATCTGCCCTTCC TGCGCCAGTTCAACCCCTTCTTCTTCTAAAAAATGATCTGCCCTTCC TGCGCCAGTTCAACCCCTTCTTCTTCTAAAAAAATGATCTGCCCTTCC TGCGCCAGTTCAACAGCCTTCTTCTTCTAAAAAAATGATCTGCCGCTTCC TGCGCCAGTTCAACAGCCTTCTTCTTCTAAAAAAAAATAAAT		CTCTCGCCGGAAGAACGCAAGGAATTTGGTCAGCGCGTCAA	
GTAGCGAGACGATCGATGTCACGCTCCCTGGCCGTGGGCAG CGACTGGGAGGACTGCACCCGGTCACGTTAACCCTCCGACG CATCACCAGGCTGTTCCGGTCACGTTGACTCTGGAGC CATCACCAGGCTGTTCCGGTCAGTTGGCTTCAGCGTCGTGG AAGGCCCGGAGATTGAAGACGACTTTCATAACTTCGAAGCCT TGAATATTCCCGCCCACCATCCGGCGCGCGCGCGCATGCAT		TCAGGCACGTGACGAGTTCCAGCGGCTCCTGGAGCGCCGC	
CGACTGGAGGACTGCACCCGGTCACGTTAACCCTCCGACG CATCACCAGGCTGTTCCGGTCAGTTGGCTTCAGCGTCGTGG AAGGCCCGAGAGATTGAAGACGACTTTCATAACTTCGAAGCCT TGAATATTCCCGCCCACCATCCGGCGCGCGCGATGCATGAC ACATTCTACTTCTCCGAACACTCCCTCCTGCGTACCCACACC AGCCCGGTCCAGATCCGCGTTATGGAGTCCGGGCAGCCCC CGCTCCGGGTGATAGCCCCCCGGACGGGTCTATCGGTGCGA CAGCGACCTGACCCACACGCCGATGTTTCACCAGGTCGAGG GCTTCTGGGTTGATGAGCACGCCGATGTTTCACCAGGTCGAAG GGCACGTTGTATGAGTTCCTTACCGGCTTCTTCGAGAAGGAC TGTGCCGTACGGTCCGACCTCTTCCGGTTCGCGGA ACCCTCGGCCGAGGTCCGACATCGAGTGCGTCATCTGCGGA GGTGATGGCTGCCGGAGCTACTTCACGGCTTGAAG GTCGGGGCTGCCGGGTATGCAAGCATTCAGGCTGGAG GCTCGGGCCGAGCTGCATCGAGGTGCGTCATCTGCGATG GTCGGGGCTGCCGGGTATGCAAGCATTCAGGCTGGCTGGA GGTGATGGGCTTGGCATGATCCATCCCCGCGTCTTCCGAGG CCGTGGGCATCGACCCCCGAACGGTATTCAGGCTTCCGCCTTC GGCCTGGGCATCGACCCCCGAACGGTATTCAGGCTTCCGCCTTC GGCCTGGGCATCCACCCCCGAACGGTATTCAGGCTTCCGCCTTCC TCACCGACCTTCCCCCTCTTCTTCGAGAATGATCTGCCGCTTCC TGCCCCAGTTCCAGCCCTTTCTTCGAGAATGATCTGCCGCTTCC TGCCCCAGTTCCAGCCCTTTCTTCGAGAATGATCTGCCGCTTCC		AAGGCGGCGCTGGAAGCCGAAGCCCTGGCACGGCGGCTGA	
CATCACCAGGCTGTTCCGGTCAGTTGGCTTCAGCGTCGG  AAGGCCCGAGAGTTGAAGACGACTTTCATAACTTCGAAGCCT  TGAATATTCCCGCCCACCACCACCGCGCGCGCGCGCGCATGCAT		GTAGCGAGACGATCGATGTCACGCTCCCTGGCCGTGGGCAG	
AAGGCCCGGAGATTGAAGACGACTTTCATAACTTCGAAGCCT TGAATATTCCCGCCCACCATCCGGCGCGCGCGCGATGCATGAC ACATTCTACTTCTCCGAACATCTCCTCCTGCGTACCCACACC AGCCCGGTCCAGATCCGGCTTATGGAGTCCGGGCAGCCCC CGCTCCGGGTGATAGCCCCCCGGACGGGTCTATCGGTGCGA CAGCGACCTGACCCACACGCCGATGTTTCACCAGGTCGAGG GCTTCTGGGTTGATGAGCAGGTGTCGTTCGCCGATCTGAAG GGCACGTTGTATGAGTTCCTTACCGGCTTCTTCGAGAAGAGAC TGTGCCGTACGGTCGACCACACTCCCGTTTTCCGGATG ACCCTCGGCCGAGGTCGACATCAACTTCCCGTTTGCGGA ACCCTCGGCCGAGGTCGACATCAAGTGCGTCATCTGCGATG GTCGGGGCTGCCGGGTATGCAAGCATTCAGGCTGGCTGAG GGTGATGGGCTTGGCATGATCCATCCCCGCGTCTTCGAGG CCGTGGGCATCGACCCCGAACGGTATTCGGGCTTCGGCTTC GGCCTGGGCGTCGAGCGCCTGACGATGCTTCCGCTTCC TGCGCCAGTTCAAGCCCTTCTTCGAGAATGATCTGCGCTTCC TGCGCCAGTTCAAGCCCTTTCTTCGAGAATGATCTGCGCTTCC TGCGCCAGTTCAAGCCCTTTCTTCGAGAATGATCTGCGCTTCC		CGACTGGGAGGACTGCACCCGGTCACGTTAACCCTCCGACG	
TGAATATTCCCGCCCACCATCCGGCGCGCGCGATGCATGAC ACATTCTACTTCTCCGAACATCTCCTCCTGCGTACCCACCC		CATCACCAGGCTGTTCCGGTCAGTTGGCTTCAGCGTCGTGG	
ACATTCTACTTCTCCGAACATCTCCTCCTGCGTACCCACACC AGCCCGGTCCAGATCCGCGTTATGGAGTCCGGGCAGCCCC CGCTCCGGGTGATAGCCCCCGGACGGGTCTATCGGTGCGA CAGCGACCTGACCCACACGCCGATGTTTCACCAGGTCGAGG GCTTCTGGGTTGATGAGCAGGTGTCGTTCGCCGATCTGAAG GGCACGTTGTATGAGTTCCTTACCGGCTTCTTCGAGAAGGAC TGTGCCGTACGGTTCCGGCCGAGCTACTTCCCGTTTGCGGA ACCCTCGGCCGAGGTCGACATCGAGTGCGTCATCTGCGATG GTCGGGGCTGCCGGGTATGCAAGCATTCAGGCTGGCTGA GGTGATGGGCTGTGGCATGATCCATCCCCGCGTCTTCGAGG CCGTGGGCATCGACCCCGAACGGTATTCAGGCTTCGGCTTC GGCCTGGGCGTCGACCCCCGAACGGTATTCGGCTTCC TCAACGACCTTCGCCTCTTCTTCGAGAATGATCTGCCCTTCC TGCGCCAGTTCAAGCCCTTCTTCTGAGAAATGATCTGCGCTTTCC TGCGCCAGTTCAAGCCCTTCTTCTGAGAAATGATCTGCGCTTTCC		AAGGCCCGGAGATTGAAGACGACTTTCATAACTTCGAAGCCT	
AGCCCGGTCCAGATCCGCGTTATGGAGTCCGGGCAGCCCC CGCTCCGGGTGATAGCCCCCGGACGGGTCTATCGGTGCGA CAGCGACCTGACCCACACGCCGATGTTTCACCAGGTCGAGG GCTTCTGGGTTGATGAGCAGGTGTCGTTCGCCGATCTGAAG GGCACGTTGTATGAGTTCCTTACCGGCTTCTTCGAGAAAGGAC TGTGCCGTACGGTTCCGGCCGAGCTACTTCCCGGTTTGCGGA ACCCTCGGCCGAGGTCGACATCGAGTGCGTCATCTGCGATG GTCGGGGCTGCCGGGTATGCAAGCATTCAGGCTGGA GGTGATGGGCTGTGGCATGATCCATCCCCGCGTCTTCGAGG CCGTGGGCATCGACCCCGAACGGTATTCCGGCTTC GGCCTGGGCGTCGACGACCGCTTCTCGAGC TCAACGACCTTCGACCCCGCTTCTCCCCCCCCTTCCC TGCGCCAGTTCAAGCCTTCCTTCCTCCGAGAATGATCCCCCCGCTTCCC TGCGCCAGTTCAAGCCCTTTCTTCGAGAATGATCTGCGCTTCC TGCGCCAGTTCAAGCCCTTTCTTCGAGAATGATCTGCGCTTCC		TGAATATTCCCGCCCACCATCCGGCGCGCGCGATGCATGAC	
CGCTCCGGGTGATAGCCCCCGGACGGGTCTATCGGTGCGA CAGCGACCTGACCCACACGCCGATGTTTCACCAGGTCGAGG GCTTCTGGGTTGATGAGCAGGTGTCGTTCGCCGATCTGAAG GGCACGTTGTATGAGTTCCTTACCGGCTTCTTCGAGAAGGAC TGTGCCGTACGGTTCCGGCCGAGCTACTTCCCGTTTGCGGA ACCCTCGGCCGAGGTCGACATCGAGTGCGTCATCTGCGATG GTCGGGGCTGCCGGGTATGCAAGCATTCAGGCTGGCTGGA GGTGATGGGCTGTGGCATGATCCATCCCCCGCGTCTTCGAGG CCGTGGGCATCGACCCCGAACGGTATTCGGGCTTCC GGCCTGGGCGTCGACCCCGAACGGTATTCGGCTTCC TCAACGACCTTCGCCTCTTCTTCGAGAATGATCTGCGCTTCC TGCGCCAGTTCAAGCCCTTCTTCTCAAaaaacgcaaagaaaatgccgatggg		ACATTCTACTTCTCCGAACATCTCCTCCTGCGTACCCACACC	
CAGCGACCTGACCCACACGCCGATGTTTCACCAGGTCGAGG GCTTCTGGGTTGATGAGCAGGTGTCGTTCGCCGATCTGAAG GGCACGTTGTATGAGTTCCTTACCGGCTTCTTCGAGAAGGAC TGTGCCGTACGGTTCCGGCCGAGCTACTTCCCGTTTGCGGA ACCCTCGGCCGAGGTCGACATCGAGTGCGTCATCTGCGATG GTCGGGGCTGCCGGGTATGCAAGCATTCAGGCTGGCTGGA GGTGATGGGCTGTGGCATGATCCATCCCCGCGTCTTCGAGG CCGTGGGCATCGACCCCGAACGGTATTCGGGCTTCC GGCCTGGGCGTCGACGCCTGACGATGCTGCCCTACGGCA TCAACGACCTTCGCCTTCTTCGAGAATGATCTGCGCTTCC TGCGCCAGTTCAAGCCCTTCTTCTTCGAGAATGATCTGCGCTTCC		AGCCCGGTCCAGATCCGCGTTATGGAGTCCGGGCAGCCCC	
GCTTCTGGGTTGATGAGCAGGTGTCGTTCGCCGATCTGAAG GGCACGTTGTATGAGTTCCTTACCGGCTTCTTCGAGAAGGAC TGTGCCGTACGGTTCCGGCCGAGCTACTTCCCGTTTGCGGA ACCCTCGGCCGAGGTCGACATCGAGTGCGTCATCTGCGATG GTCGGGGCTGCCGGGTATGCAAGCATTCAGGCTGGCTGGA GGTGATGGGCTGTGGCATGATCCATCCCCGCGTCTTCGAGG CCGTGGGCATCGACCCCGAACGGTATTCGGGCTTCC GGCCTGGGCGTCGACCCCTGACGATGCTCCCCGCTTCC TCAACGACCTTCCTCTCTCGAGAATGATCTGCGCTTCC TGCGCCAGTTCAACGCCTTCTTCTCGAGAATGATCTGCGCTTCC		CGCTCCGGGTGATAGCCCCCGGACGGGTCTATCGGTGCGA	
GGCACGTTGTATGAGTTCCTTACCGGCTTCTTCGAGAAGGAC TGTGCCGTACGGTTCCGGCCGAGCTACTTCCCGTTTGCGGA ACCCTCGGCCGAGGTCGACATCGAGTGCGTCATCTGCGATG GTCGGGGCTGCCGGGTATGCAAGCATTCAGGCTGGCTGGA GGTGATGGGCTGTGGCATGCATCCCCCGCGTCTTCGAGG CCGTGGGCATCGACCCCGAACGGTATTCGGGCTTCC GGCCTGGGCGTCGAGCGCCTGACGATGCTGCGCTTC TCAACGACCTTCCTCTTCTCGAGAATGATCTGCGCTTCC TGCGCCAGTTCAAGCCCCTTCTTCTGAGAAATGATCTGCGCTTCC		CAGCGACCTGACCCACACGCCGATGTTTCACCAGGTCGAGG	
TGTGCCGTACGGTTCCGGCCGAGCTACTTCCCGTTTGCGGA ACCCTCGGCCGAGGTCGACATCGAGTGCGTCATCTGCGATG GTCGGGGCTGCCGGGTATGCAAGCATTCAGGCTGGCTGGA GGTGATGGGCTGTGGCATGATCCATCCCCGCGTCTTCGAGG CCGTGGGCATCGACCCCGAACGGTATTCGGGCTTCC GGCCTGGGCGTCGAGCGCCTGACGATGCTGCGCTTCC TCAACGACCTTCGCCTTCTTCGAGAATGATCTGCGCTTCC TGCGCCAGTTCAAGCCCCTTCTTCTGAaaaacgcaaagaaaatgccgatggg		GCTTCTGGGTTGATGAGCAGGTGTCGTTCGCCGATCTGAAG	
ACCCTCGGCCGAGGTCGACATCGAGTGCGTCATCTGCGATG GTCGGGGCTGCCGGGTATGCAAGCATTCAGGCTGGA GGTGATGGGCTGTGGCATGATCCATCCCCGCGTCTTCGAGG CCGTGGGCATCGACCCCGAACGGTATTCGGGCTTCC GGCCTGGGCGTCGAGCGCTGACGATGCTGCGCTACGGCA TCAACGACCTTCGCCTTCTTCGAGAATGATCTGCGCTTCC TGCGCCAGTTCAAGCCCTTCTTGAaaaacgcaaagaaaatgccgatggg		GGCACGTTGTATGAGTTCCTTACCGGCTTCTTCGAGAAGGAC	
GTCGGGGCTGCCGGGTATGCAAGCATTCAGGCTGGCTGGA GGTGATGGGCTGGCATGATCCATCCCCGCGTCTTCGAGG CCGTGGGCATCGACCCCGAACGGTATTCGGGCTTCGGCTTC GGCCTGGGCGTCGAGCGCCTGACGATGCTGCGCTACGGCA TCAACGACCTTCGCCTCTTCTTCGAGAATGATCTGCGCTTCC TGCGCCAGTTCAAGCCCCTTCTGAaaaacgcaaagaaaatgccgatggg		TGTGCCGTACGGTTCCGGCCGAGCTACTTCCCGTTTGCGGA	
GGTGATGGGCTGTGGCATGATCCATCCCCGCGTCTTCGAGG CCGTGGGCATCGACCCCGAACGGTATTCGGGCTTCGGCTTC GGCCTGGGCGTCGAGCGCCTGACGATGCTGCGCTACGGCA TCAACGACCTTCGCCTCTTCTTCGAGAATGATCTGCGCTTCC TGCGCCAGTTCAAGCCCTTCTGAaaaacgcaaagaaaatgccgatggg		ACCCTCGGCCGAGGTCGACATCGAGTGCGTCATCTGCGATG	
CCGTGGGCATCGACCCCGAACGGTATTCGGGCTTCGGCTTC GGCCTGGGCGTCGAGCGCCTGACGATGCTGCGCTACGGCA TCAACGACCTTCGCCTCTTCTTCGAGAATGATCTGCGCTTCC TGCGCCAGTTCAAGCCCTTCTGAaaaacgcaaagaaaatgccgatggg		GTCGGGGCTGCCGGGTATGCAAGCATTCAGGCTGGCTGGA	
GGCCTGGGCGTCGAGGCCCTGACGATGCTGCGCTACGGCA TCAACGACCTTCGCCTCTTCTTCGAGAATGATCTGCGCTTCC TGCGCCAGTTCAAGCCCTTCTGAaaaacgcaaagaaaatgccgatggg		GGTGATGGGCTGTGGCATGATCCATCCCCGCGTCTTCGAGG	
TCAACGACCTTCGCCTCTTCTTCGAGAATGATCTGCGCTTCC TGCGCCAGTTCAAGCCCTTCTGAaaaacgcaaagaaaatgccgatggg		CCGTGGGCATCGACCCCGAACGGTATTCGGGCTTCGGCTTC	
TGCGCCAGTTCAAGCCCTTCTGAaaaacgcaaagaaaatgccgatggg		GGCCTGGGCGTCGAGCGCCTGACGATGCTGCGCTACGGCA	
		TCAACGACCTTCGCCTCTTCTTCGAGAATGATCTGCGCTTCC	
capsulatus carbonic anhydrase (CA) knockouts		TGCGCCAGTTCAAGCCCTTCTGAaaaacgcaaagaaaatgccgatggg	
	1. capsulatus carbonic anhydrase (CA) kr	nockouts	

CAH723 MCA1442KO 1kbUP F		Amendify 1 Made are also as from - A4
	acagctatgacatgattacgaattcTCGATGGCGGGATCGTCTTG	Amplify 1 Kb homology from <i>M</i> .
CAH063 MCA1442KO 1kbUP R	gatccccaattcgGAGTTCGCTCTTAGGTTTTGAAAGG	capsulatus upstream of MCA1442
CAH064 FRT-Gm F	aagagcgaactcCGAATTGGGGATCTTGAAG	Amplify 1.2 Kb Gm <sup>R</sup> cassette from
CAH065 FRT-Gm R	caggtcagccgcCGAATTAGCTTCAAAAGC	pPS856
CAH066 MCA1442KO 1kbDN F	tgaagctaattcgGCGGCTGACCTGGTCTTC	Amplify 1 Kb homology from <i>M</i> .
CAH724 MCA1422KO 1kbDN R	taaaacgacggccagtgccaagcttTCTCCGGTGGATGCCGCC	capsulatus downstream of MCA1442
CAH129 MCA1442KO flank F	CCGCCTTTCCAAAACC	Confirm MCA1442 knockout
CAH130 MCA1442KO flank R	TGAAGACCAGGTCAGCCG	
CAH725 MCA1665KO 1kbUP F	acagctatgacatgattacgaattcATATGTCACAATCCGCTTC	Amplify 1 Kb homology from M.
CAH069 MCA1665KO 1kbUP R	agctccagcctacacGATTTCTGTCCTTGATAAGG	capsulatus upstream of MCA1665
CAH070 FRT-Kn F	aggacagaaatcGTGTAGGCTGGAGCTGCTTC	Amplify 1 Kb Kn <sup>R</sup> cassette from pKD13
CAH071 FRT-Kn R	acaggcaagaaCTGTCAAACATGAGAATTAATTCCGG	
CAH072 1665KO 1kbDN F	tctcatgtttgacagTTCTTGCCTGTGACCGATTG	Amplify 1 Kb homology from M.
CAH726 1665KO 1kbDN R	taaaacgacggccagtgccaagcttATGTGGCGGCTAGTACAG	capsulatus downstream of MCA1665
CAH131 MCA1665KO flank F	GCATCCACCTTATCAAGGACAGAA	Confirm MCA1665 knockout
CAH132 MCA1665KO flank R	TTCTCGGGCCGCTTCATC	
CAH727 MCA2797KO 1kbUP F	acagctatgacatgattacgaattcATCCTCGATTTCGAAGATGG	Amplify 1 Kb homology from <i>M</i> .
CAH075 MCA2797KO 1kbUP R	gatccccaattcgCTTTCCTCTCTGCCGGTC	capsulatus upstream of MCA2797
CAH076 FRT-Gm F	cagagaggaaagCGAATTGGGGATCTTGAAG	Amplify 1.2 Kb Gm <sup>R</sup> cassette from
CAH077 FRT-Gm R	gcgcatgttgggCGAATTAGCTTCAAAAGC	pPS856
CAH078 MCA2797KO 1kbDN F	tgaagctaattcgCCCAACATGCGCAAGACTC	Amplify 1 Kb homology from M.
CAH728 MCA2797KO 1kbDN R	taaaacgacggccagtgccaagcttCGTGACGGTGACGTTATTG	capsulatus downstream of MCA2792
CAH133 MCA2797KO flank F	CGACCGGCAGAGAGAAAG	Confirm MCA2797 knockout
CAH134 MCA2797KO flank R	GAGTCTTGCGCATGTTGGG	
CAH729 MCA0910KO 1kbUP F	acagctatgacatgattacgaattcGCCCTGCATGTATGAACC	Amplify 1 Kb homology from M.
		capsulatus upstream of MCA0910

(Continued on next page)

 TABLE 2
 Synthetic DNA and primers<sup>a</sup> (Continued)

Fragment/Primer name	Sequence	Purpose	
CAH081 MCA0910KO 1kbUP R	agctccagcctacacCGTGTATATCTCCTCTGGG		
CAH082 FRT-Kn F	gagatatacacgGTGTAGGCTGGAGCTGCTTC	Amplify 1 Kb Kn <sup>R</sup> cassette from pKD13	
CAH083 FRT-Kn R	ggtcgccacggcCTGTCAAACATGAGAATTAATTCCGG		
CAH084 MCA0910KO 1kbDN F	tctcatgtttgacagGCCGTGGCGACCTCGAAAG	Amplify 1 Kb homology from M.	
CAH730 MCA0910KO 1kbDN R	taaaacgacggccagtgccaagcttCCCTGGTCGAAGCAGGCG	capsulatus downstream of MCA0910	
CAH135 MCA0910 flank F	ACACAACCCAGAGGAGATATACACG	Confirm MCA0910 knockout	
CAH136 MCA0910 flank R	TGATTGGCCTCTGCGAAGAAA		
CAH731 MCA1080KO 1kbUP F	acagctatgacatgattacgaattcCGTCCCGCAGTTCCGCCG	Amplify 1 Kb homology from M.	
CAH087 MCA1080KO 1kbUP R	gatccccaattcgCCCAATTCCTCCCTTCAACGGC	capsulatus upstream of MCA1080	
CAH088 FRT-Gm F	ggaggaattgggCGAATTGGGGATCTTGAAG	Amplify 1.2 Kb Gm <sup>R</sup> cassette from	
CAH089 FRT-Gm R	gacgattcgtgaCGAATTAGCTTCAAAAGC	pPS856	
CAH090 MCA1080KO 1kbDN F	tgaagctaattcgTCACGAATCGTCCCCTCC	Amplify 1 Kb homology from <i>M</i> .	
CAH732 MCA1080KO 1kbDN R	taaaacgacggccagtgccaagcttGGCGATCTTATTTGCTCGAAG	capsulatus downstream of MCA1080	
CAH137 MCA1080 flank F	CCGTTGAAGGGAGGAATTGGG	Confirm MCA1080 knockout	
CAH138 MCA1080 flank R	TTTGGCCTGCGCGTTAAAC		
CAH572 pK18mobsacB F	AAACGCAAAAGAAAATGC	Linearize pK18mobsacB for pK18mob-	
CAH573 pK18mobsacB R	CGTTCATGTCTCCTTTTTTATG	pheS construction	
CAH576 pK18mobpheS F	AAGCTTGGCACTGGCCGT	Linearize pK18mobpheS for knockout	
CAH577 pK18mobpheS R	GAATTCGTAATCATGTCATAGCTGTTTCCTG	construction	
CAH618 pK18mobpheS seq F	TGTTGTGGGAATTGTGAGC	Sequencing primers for pK18mobpheS	
CAH619 pK18mobpheS seq R	GATGTGCAAGGCGATTA	constructs	
M. capsulatus CA overexpression	difficultividedini in	constructs	
CAH169 MCA1422 F	gtgatagagaaaagtgaaATGGAAGCTTTCGAGCGAATG	Amplify 645 bp MCA1422 ORF for	
CAH170 MCA1422 R	cttcacaggtcaagcttCTATTCGGAGAAATCGACGTAC	overexpression construct	
CAH171 MCA1665 F	gtgatagagaaaagtgaaGTGCAAGAGTCTGACAGC	Amplify 717 bp MCA1665 ORF for	
CAH171 MCA1665 R			
CAH172 MCA1003 K CAH173 MCA2797 F	cttcacaggtcaagcttTCAATCGGTCACAGGCAAG	overexpression construct	
CAH174 MCA2797 R	gtgatagagaaaagtgaaATGGCGGTCTCGC	Amplify 543 bp MCA2797 ORF for	
	cttcacaggtcaagcttCTAAGCGGGCTCTGCC	overexpression construct	
CAH175 MCA0910 F	gtgatagagaaaagtgaaATGTCACAGATTCTCAGCGAAGTACTG	Amplify 579 bp MCA0910 ORF for	
CAH176 MCA10910 R	cttcacaggtcaagcttCTAAGCGGCTCTGCCCGC	overexpression construct	
CAH177 MCA1080 F CAH178 MCA1080 R	gtgatagagaaaagtgaaATGGTACGGCGAACCATTTG	Amplify 795 bp MCA1080 ORF for	
	cttcacaggtcaagcttTCACGGATCGACGTTCCTG TCACGGATCGACGTTCCTG	overexpression construct Pair with oCAH004 to linearize pCA2	
CAH1426 MCA1080 R	TCACGGATCGACGTTCCTG	•	
CAH1431 MCA1422 F	cgatccgtgaAACCTAAGAGCGAACTCATG	and insert MCA1422 with native RBS  Pair with oCAH170 to amplify MCA1422	
		with native RBS	
CAH003 pCAH01 R	TTCACTTTTCTCTATCACTGATAG	Linearize pCAH01 for CA overexpression	
CAH004 pCAH01 F	AAGCTTGACCTGTGAAGTG	construction	
CAH005 pCAH01 seq F	CCCGACACCATCGAATGGCCAGATG	Sequencing primers for overexpression	
CAH006 pCAH01 seq R	AGGGCGCGTGGAGATCCGT	constructs	
M. capsulatus CA qRT-PCR			
CAH350 MCA0910 RT F	TGTCACAGATTCTCAGCGAAG	qRT-PCR primers for MCA0910	
CAH351 MCA0910 RT R	TCCATGCAGGTCAATATAGCG	·	
CAH352 MCA1080 RT F	ACCTTATCAACATCCACGAGC	qRT-PCR primers for MCA1080	
CAH353 MCA1080 RT R	TCTGCTTGTTCTGATGGACG	· ·	
CAH344 MCA1442 RT F	AACAAATGGCTGAAACACGTC	qRT-PCR primers for MCA1442	
CAH345 MCA1442 RT R	GTGGGCCAGATTGTATACCTG	q r en printers for ment 1412	
CAH346 MCA1665 RT F	CAGCAAAGGCAAGGATGAATG	qRT-PCR primers for MCA1665	
CAH347 MCA1665 RT R	TCCTTGAATCCTTTGACGCC	q.c. i en primers for mercroos	
CAH348 MCA2797 RT F	CACTGAAGGACTCCGAACTC	gRT-PCR primers for MCA2797	
CAH 349 MCA2797 RT R	CGCAAATACCGCTCCTTTAG	qui i en primers for MCA2737	
CALL 343 INICAZ/3/ NT N	COCANAIACCOCTCCTTIAG		

 $<sup>{}^{</sup>a}\text{Lowercase bases represent homology arms for isothermal assembly.}$ 

Overexpression plasmids and strains were created by amplifying each CA open reading frame from *M. capsulatus* Bath gDNA using the corresponding primers (oCAH169-oCAH178) and assembling with pCAH01 linearized *via* PCR with primers oCAH3/oCAH4 to create pCA1-pCA5, placing the genes under transcriptional control of the anhydrotetracycline (aTc)-inducible P<sub>tet</sub> promoter. To generate the pCA2/3 plasmid for co-expression of CA2 and CA3, the CA3 ORF with its native ribosome binding site was amplified from gDNA with primers oCAH1431/oCAH170 and assembled with pCA2 linearized with primers oCAH1424/oCAH4, generating a CA2-CA3 operon. Overexpression constructs were then transferred to *M. capsulatus* Bath *via* biparental mating. Antibiotic-resistant *M. capsulatus* transformants were screened *via* colony PCR using plasmid-specific primers oCAH5/oCAH6 and the resultant PCR amplicon sequence was verified *via* Sanger sequencing.

### CA alignment and phylogenetic analysis

The *M. capsulatus* CA protein sequences were aligned to respective homologous CA sequences with solved structures using Geneious Prime. Other CA homologs were identified in the NCBI database *via* BlastP using a standard BLOSUM62 matrix. Methanotroph CA homologs were identified in the NCBI database limiting the search to include Methylococcaceae, Methylothermaceae, Methylocystaceae, and Beijerinckiaceae methanotroph-containing families and excluding the *Methylococcus* genus. Distance trees of the top hits with query coverage  $\geq$ 80% and E values  $\leq$  1e<sup>-30</sup> were constructed with NCBI Blast Tree using a Fast Minimum Evolution method.

### CA activity assay

Wild-type M. capsulatus Bath cultivated in 10 mL liquid NMS to  $OD_{600} \sim 1.0$  were pelleted at  $4,080 \times g$  for 10 minutes, and the supernatant was removed via aspiration. Cells were lysed using the B-PER bacterial protein extraction reagent (Thermo-Fisher) and total protein was quantified on a Nanodrop spectrophotometer using the Pierce  $660_{nm}$  Protein Assay Reagent (Thermo-Fisher) compared to known BSA standards. Lysates were normalized to 10 mg/mL protein in 10 mM Tris HCl, and 100  $\mu$ g of lysate was used to determine CA activity following the Abcam Carbonic Anhydrase Colorimetric Activity Assay Kit protocol (Abcam). Briefly, cell lysate and kit reagents were added to microtiter plates and allowed to incubate for 10 minutes at room temperature covered/protected from light and then production of nitrophenol was monitored at  $A_{405nm}$  every 30 seconds for 10 minutes using a BioTek Synergy Mx microplate reader. Nitrophenol was quantified via regression analysis compared to known nitrophenol standards which correlates to CA activity based on activity curves previously generated by the manufacturer. Acetazolamide (AZM) was added to a final concentration of 100  $\mu$ M to inhibit CA activity in reactions where indicated.

### **AZM** treatment

Wild-type or AZM-adapted M. capsulatus Bath were grown in a liquid medium to  $OD_{600} \sim 1$  and diluted to  $OD_{600} = 0.1$  in fresh medium with or without AZM (Sigma-Aldrich). Cell death and/or growth was monitored via dilution plating and spectrophotometrically at  $OD_{600}$  using a Nanodrop spectrophotometer. % killing was calculated by comparing the colony forming units (CFUs) after treatment to CFUs at T = 0.

### CA transcription analysis via quantitative reverse-transcriptase PCR

CA transcription was determined in wild-type M. capsulatus cultivated in serum vials or a continuous gas bioreactor. Serum vial seed cultures were inoculated to  $OD_{600} = 0.1$  in liquid NMS from plate biomass and cultivated for 24 h. Seed cultures were diluted in fresh medium to  $OD_{600} = 0.01$  (serum vials) or  $OD_{600} = 0.1$  (bioreactor). Serum vial cultivations were grown until the mid-log phase ( $OD_{600} = 0.5$ ) for RNA extraction. To evaluate CA transcription in response to  $CO_2$  starvation, bioreactor cultures were

cultivated with continuous 20% CH<sub>4</sub>/2% CO<sub>2</sub> in the air for 3 h (CO<sub>2</sub>-replete) after which the gas composition was switched to 20% CH<sub>4</sub> in the air (CO<sub>2</sub>-deplete) and cells were cultivated for an additional 3 h prior to RNA extraction. Cell cultures were mixed 5:1 with ice-cold 5% phenol/95% ethanol and incubated for 20 minutes on ice prior to RNA isolation using the High Pure RNA Isolation Kit with optional on-column DNase treatment (Roche). Total RNA (1  $\mu$ g) was used to generate cDNA using the Superscript Vilo IV reverse transcriptase kit following the manufacturer's protocol (Invitrogen). Primers used for qPCR are listed in Table 2. Reactions were prepared using Powertrack SYBR Green master mix (Applied Biosystems) using recommended cycling conditions and amplification detection with a QuantStudio 3 qPCR system. Expression of each CA determined by cycle threshold (Ct) was normalized to the housekeeping gene rpoD and relative expression between targets or conditions was calculated using the  $\Delta\Delta$ Ct method.

### Gas chromatography and biomass yield calculations

Wild-type M. capsulatus and overexpression strains (pCA1-pCA5) were grown overnight in a liquid medium (OD $_{600}$  ~0.1) with 50 µg/mL kanamycin and 0.2 µg/mL aTc for CA induction, where applicable. Seed cultures were sub-cultured to  $OD_{600} = 0.1$  in fresh medium without antibiotics (to avoid any growth inhibition) and 0.2 μg/mL aTc for CA induction in serum vials, which were stoppered, sealed, and 20% CH<sub>4</sub> added to the headspace via syringe. The CH<sub>4</sub> and CO<sub>2</sub> composition in the headspace was determined 10 min after gas addition and every 24 h during methanotroph cultivation using an SRI 8610 c gas chromatograph combined with an SRI S.S HayeSep D  $6' \times 1/8''$  column, SRI on-column injector, and TCD and FID detectors (SRI Instruments). Runs were 3 minutes in length, isocratic at 50°C. Gases were quantified as % composition by comparison to known standards. % gas was converted to weight using the specific gravities of CH<sub>4</sub> (0.622 mg/mL) or CO<sub>2</sub> (1.47 mg/mL) at 37°C. CH<sub>4</sub> uptake and CO<sub>2</sub> evolution rates per dry cell weight (DCW) were determined by converting OD<sub>600</sub> to DCW using a formula empirically determined by comparing OD<sub>600</sub> measurements to colony forming units during serum vial cultivation (OD<sub>600</sub> = 1 is equivalent to 0.254  $\pm$  0.0249 g DCW/L). The biomass yield/carbon conversion efficiency (CCE) at the late logarithmic growth phase (48 h) was calculated using the following equation: g DCW/(mmol CO2 evolved/mmol CH<sub>4</sub> consumed).

### Competitive growth index

Wild-type M. capsulatus and antibiotic-resistant CA overexpression strains were equally mixed/subcultured to  $OD_{600} \sim 0.01$  in NMS liquid medium and cultured for 48 h to late logarithmic phase. Serial dilutions of the cultures were replica plated on NMS and NMS containing 50  $\mu$ g/mL kanamycin before and after cultivation, and CFUs were enumerated after 1 week of incubation. Competitive indices were calculated by determining the ratio of CA-overexpression strain CFUs to wild-type CFUs after cultivation (output ratio) divided by the CFU inoculum ratio (input ratio) using the following equation: output ratio [NMS Kn CFUs- (NMS CFUs - NMS Kn CFUs)] / input ratio [NMS Kn CFUs - (NMS CFUs - NMS Kn CFUs)].

### Statistical analysis

Statistical analysis was performed using GraphPad Prism 10 software. The data between the two groups were analyzed using unpaired t-tests. The determination of statistical significance between multiple comparisons was achieved using analysis of variance (ANOVA) followed by Dunnett's multiple comparisons test. Data were considered statistically significant when  $P \le 0.05$ .

Month XXXX Volume 0 Issue 0 10.1128/msphere.00496-24 **8** 

### **RESULTS**

### M. capsulatus Bath encodes five carbonic anhydrase isoforms

Five CA-encoding genes are annotated in the M. capsulatus Bath genome: MCA0910 (CA1), MCA1080 (CA2), MCA1442 (CA3), MCA1665 (CA4), and MCA2797 (CA5). The genes encode  $\alpha$ -(CA2),  $\gamma$ -(CA5), and  $\beta$ -CAs (CA1, clade D; CA3, clade A, CA4, clade B) with limited amino acid sequence identity (Fig. 1A), but have well-conserved features to known CA families (Fig. S1 to S5) (27, 44–46). Phylogenetic analyses indicate that  $\beta$ -CA1,  $\beta$ -CA3, and γ-CA5 are highly conserved in methanotrophic bacteria, and the CA phylogenetic trees are congruent with 16s- and pmoA-based methanotroph classifications (8) (Fig. S6, S8, S10, S11, S13 and S15; supplemental table file S1 and S2). By contrast,  $\alpha$ -CA2 and  $\beta$ -CA4 isoform orthologs share limited sequence identity (<30%) with other methanotroph CAs (Fig. S7, S9, S12, and S14; supplemental table file S2), while orthologs in non-methanotrophic bacteria with higher sequence identity (>50%) were identified, suggesting these isoforms may have been acquired via horizontal gene transfer. The phylogenetic analysis of the M. capsulatus α-CA2 identified orthologs in phylogenetically diverse phototrophic green non-sulfur bacteria, purple sulfur bacteria, and chemolithoautotrophic bacteria (Fig. S2 Fig. S7; File. S1). Furthermore, α-CA2, but not the other isoforms, contains a predicted Sec-specific signal sequence identified by SignalP (47), suggesting that this

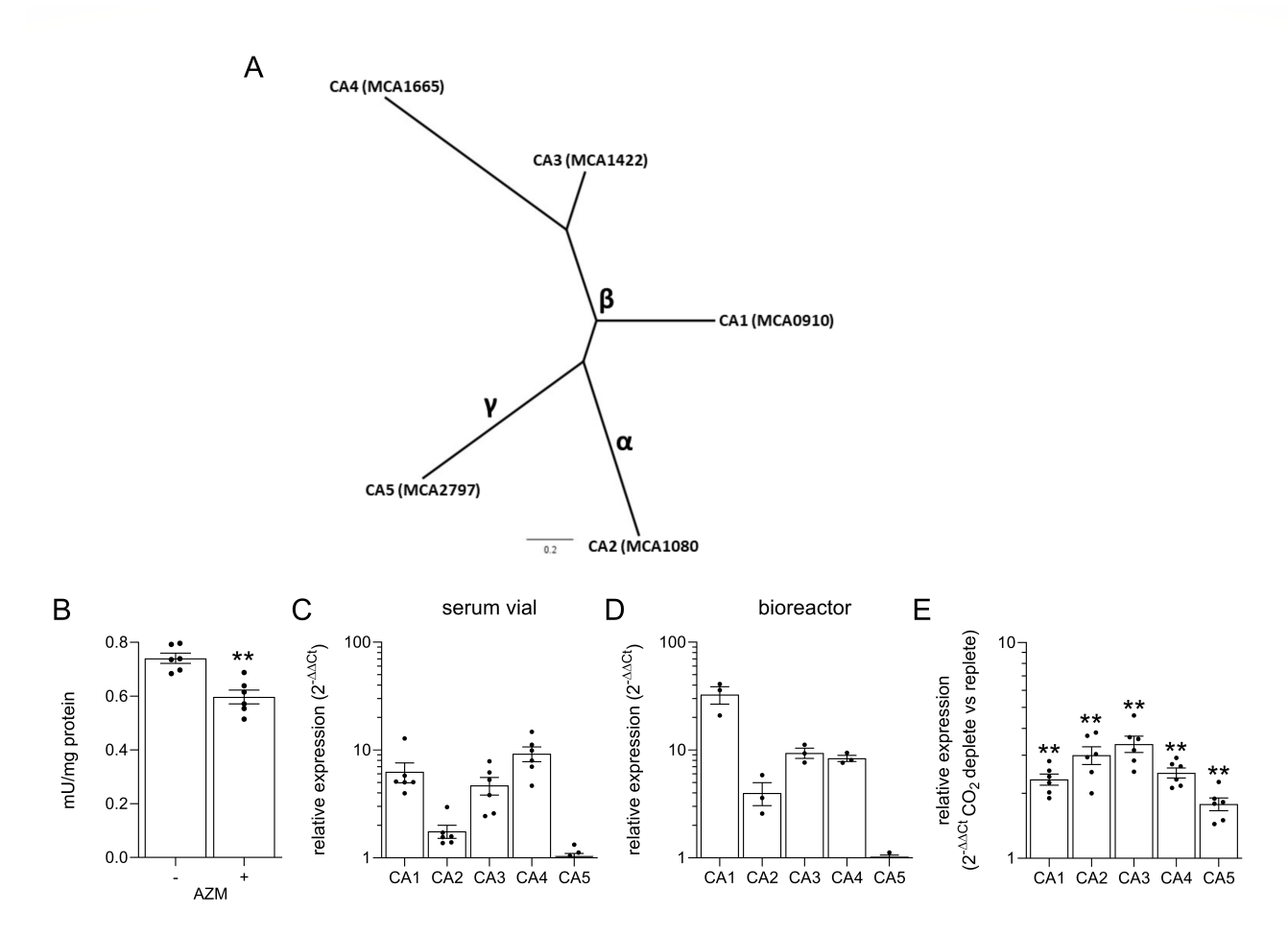


FIG 1 *M. capsulatus* expresses five CA isoforms. (A) Phylogenetic tree of the five annotated CAs encoded by the *M. capsulatus* Bath genome. Locus tags are indicated in parentheses. The scale bar represents substitutions per site. (B) CA activity was measured in whole-cell lysates in the presence (+) or absence (–) of the CA inhibitor acetazolamide (AZM). Relative transcription of the CA isoforms determined by qRT-PCR during *M. capsulatus* cultivation in (C) serum vials with 20% CH<sub>4</sub> in air or (D) a gas reactor supplied with a continuous mixture of 20% CH<sub>4</sub>/2% CO<sub>2</sub> in air. (E) Relative CA transcription a a continuous gas reactor 3 h after CO<sub>2</sub> depletion from the gas mixture. Data in B–E represent the mean  $\pm$  SEM from at least two independent experiments (n = 3-6). \*\* $P \le 0.01$ .

CA is secreted to the periplasm. CA activity can be detected in M. capsulatus whole-cell lysates (0.74  $\pm$  0.05 mU/mg protein), which could be partially inhibited by the carbonic anhydrase inhibitor acetazolamide (AZM, Fig. 1B). The CA activity assay we used is based on the ability of CA to hydrolyze p-nitrophenol acetate. Thus, the limited (20%) decrease in CA activity we observed after AZM treatment may be explained by (i) most of the activity is due to non-CA esterases in the cell lysate or (ii) the majority of M. capsulatus CA activity is AZM-resistant.

Quantitative real-time PCR established that all CA isoforms were transcribed during bacterial cultivation in a serum vial with CH<sub>4</sub> as the only supplied carbon source and in a bioreactor with continuous CH<sub>4</sub> and CO<sub>2</sub> supply (Fig. 1C and D).  $\beta$ -CA4 showed the highest relative expression in serum vials, which was 9.3-fold higher than the lowest expressed  $\gamma$ -CA5. Relative expression of  $\beta$ -CA1 was 3.6-fold higher (P < 0.05) in a bioreactor culture compared to a serum vial, but the expression of the other CA genes was comparable between these two growth conditions (Fig. 1C). The difference in expression between the highest ( $\beta$ -CA1) and lowest ( $\gamma$ -CA5) expressed CA genes was 32.7-fold in bioreactor-grown cells (Fig. 1D). To evaluate whether *M. capsulatus* Bath regulates CA expression in response to CO<sub>2</sub> availability, we compared CA transcription in bioreactor-cultivated cells after the removal of CO<sub>2</sub> from the gas stream (CO<sub>2</sub>-deplete) to those cultured with continuous 20% CH<sub>4</sub> and 2% CO<sub>2</sub> in air (CO<sub>2</sub>-replete) (Fig. 1E). In support of the role of the CAs in CO<sub>2</sub> metabolism, transcription of all isoform genes was significantly increased within 3 h after CO<sub>2</sub> starvation (CA1 2.6-fold; CA2 3.4-fold; CA3 3.8-fold; CA4 2.8-fold, and CA5 2.0-fold).

# The carbonic anhydrase inhibitor acetazolamide inhibits $\it M.~ cap sulatus$ growth

The importance of CA activity for bacterial growth was initially tested by treating cells with increasing concentrations of AZM. AZM showed dose-dependent M. capsulatus growth inhibition with 100 µM AZM-treated cultures exhibiting a 3-day lag phase followed by growth with similar kinetics to untreated cells (open circles, Fig. 2A). Dilution plating of AZM-treated cells supported that the CA inhibitor is bactericidal, killing 98% of the treated cells within 72 h after exposure (Fig. 2B). However, a population of cells survived and began to expand after 96 h (Fig. 2B), which was not due to AZM degradation given that AZM maintains its growth inhibitory effect after abiotic incubation in NMS medium at 37°C for up to 10 days (data not shown). We did not rule out the possibility that AZM was biologically consumed or degraded under our experimental conditions. However, the hyper resistance of AZM-treated cells to AZM concentrations that completely inhibited the growth of naïve controls indicated that M. capsulatus adapts to overcome AZM-mediated toxicity (Fig. 2C). To test whether the CAs may be related to the AZM adaptation, we quantified CA transcription in 10 independent colonies from the AZM-adapted population and found that each strain showed increased overall CA expression ranging from 6.8- to 25.8-fold compared to collective wild-type CA expression levels (Fig. 2D), linking AZM resistance to increased CA expression. However, there was variation between which CA isoforms were induced, and to what extent, in the adapted strains preventing a direct correlation of AZM resistance to a particular CA isoform (Fig. 2E).

### Carbonic anhydrase mutants exhibit defective growth

To assess the role of the individual CAs, we constructed five CA-deficient strains lacking each individual CA isoform *via* marker-exchange mutagenesis (ΔCA1::Kn<sup>R</sup>, ΔCA2::Gm<sup>R</sup>, ΔCA3::Gm<sup>R</sup>, ΔCA4::Kn<sup>R</sup>, and ΔCA5::Gm<sup>R</sup>). Antibiotic-resistant transformants were isolated on solid NMS medium and individual CA knock-out strains were confirmed *via* PCR (Fig. 3A). These CA knock-out transformants appeared after 4–8 weeks of incubation compared to isogenic wild-type *M. capsulatus* Bath that formed visible colonies within 1–2 weeks, underscoring that each CA isoform has a critical, non-redundant role in *M. capsulatus* metabolism and physiology. The extreme growth defects of the CA knock-out

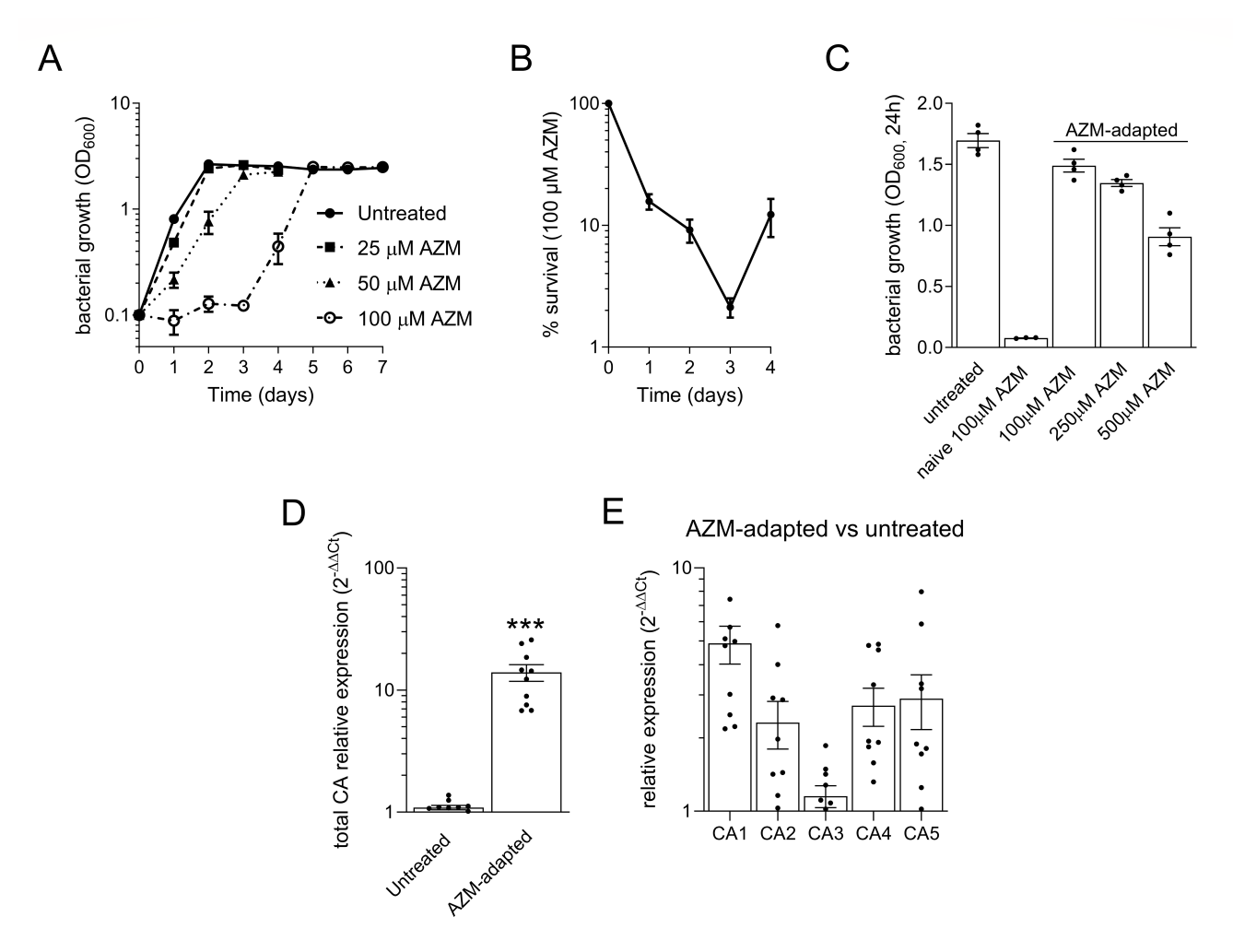


FIG 2 *M. capsulatus* is hypersusceptible to carbonic anhydrase inhibition. (A) Bacterial growth in liquid NMS medium with the acetazolamide (AZM) CA inhibitor compared to an untreated control. (B) Survival of *M. capsulatus* after exposure to 100  $\mu$ M AZM. (C) Bacterial growth of AZM-adapted cells in the presence of AZM compared to naïve and untreated controls. Collective (D) or individual (E) CA transcription in 10 AZM-adapted transformants compared to wild-type controls was evaluated using qRT-PCR. The data represent the mean  $\pm$  SEM from at least two independent experiments (n = 3-10). \*\*\* $P \le 0.001$ .

strains precluded reasonable growth comparison in liquid NMS medium; thus, we spotted dilution series of plate-derived wild-type and CA KO M. capsulatus strains on solid medium (Fig. 3B). After 10 days of incubation, wild-type colonies were readily visible, but the CA KO strains had no observable growth, even in the undiluted spots (Fig. 3B). We introduced a plasmid with tetracycline promoter ( $P_{\text{tet}}$ )/aTc-inducible expression of a CA into its respective CA KO background strain to confirm that the observed growth defects were attributed to the removal of the CA and not unintended genetic defects. Growth defects were complemented by ectopic expression of CA2, CA3, and CA5 in strains pCA2  $\Delta$ CA2::Gm<sup>R</sup>, pCA3  $\Delta$ CA3::Gm<sup>R</sup>, and pCA5  $\Delta$ CA5::Gm<sup>R</sup>, respectively (Fig. 3C). However, we were unable to recover growth of ΔCA1::Kn<sup>R</sup> and ΔCA4::Kn<sup>R</sup> strains, potentially due to dysregulated expression of CA1 or CA4 from the pCAH01 Ptet promoter or off-target effects resulting from removal of the CA gene. An 86-bp intergenic region exists between CA1 and the downstream gene and CA4 appears to be the first gene in an operon with a downstream gene (the CA4 stop codon and downstream MCA1664 start codon are separated by 11 bp). However, the putative ribosomal binding site at the 3' ends of the CA4 open reading frame was maintained in the  $\Delta$ CA4::Kn<sup>R</sup> strain to ensure translation of the downstream gene transcript, but it is possible that removal of the CA1 or CA4 sequences could disrupt regulatory elements that control the expression

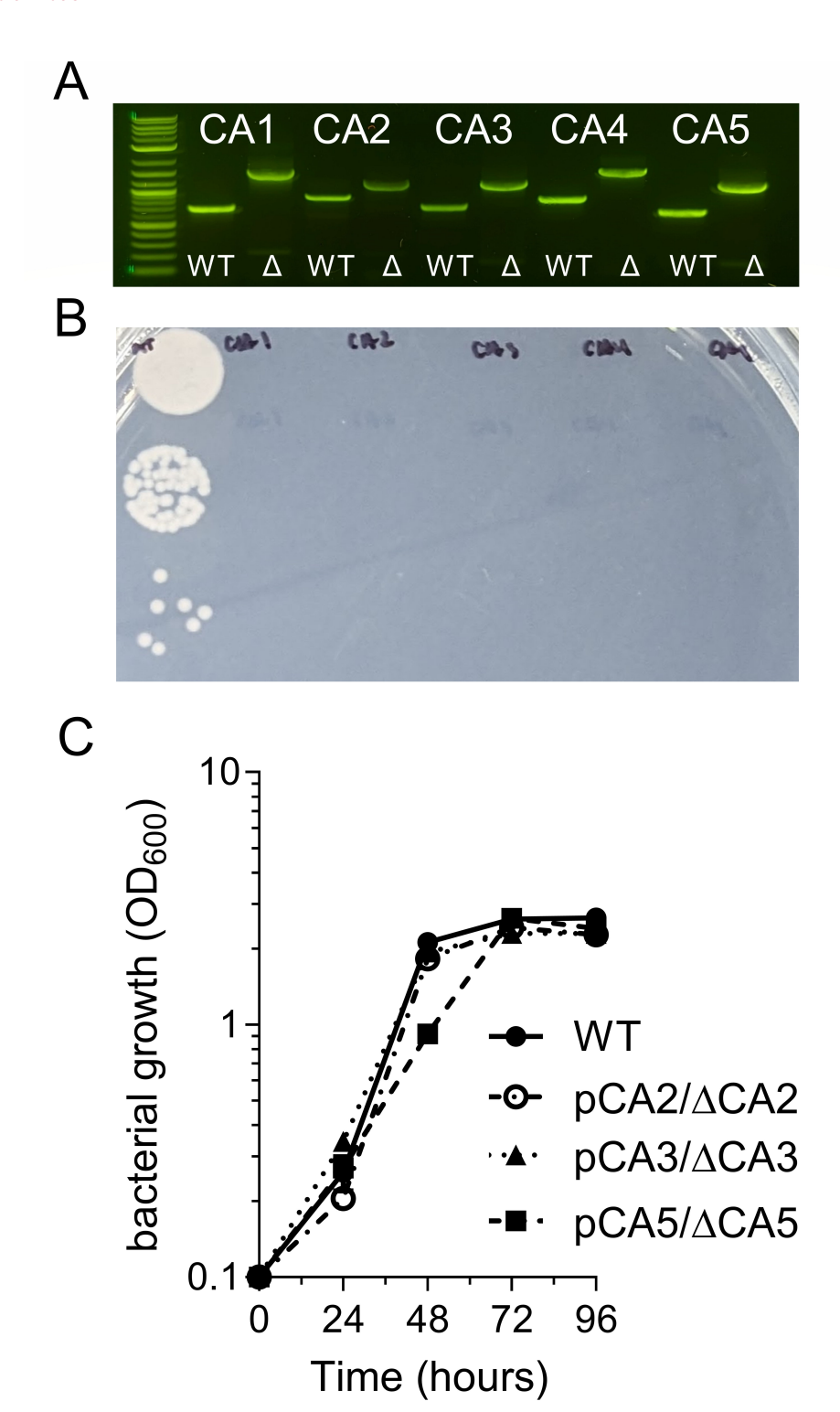


FIG 3 CA-deficient *M. capsulatus* exhibits defective growth. (A) Confirmation of individual CA knock-out strains *via* PCR. CA genes were replaced with antibiotic resistance cassettes *via* marker-exchange mutagenesis and knock-out (Δ) strains were confirmed *via* PCR compared to WT. (B) Comparison of colony formation 1 week after incubation of a dilution plate of equivalent WT and CA knock-out strains (CA1-5). (C) Bacterial growth of wild-type and ΔCA2, ΔCA3, and ΔCA5 knock-out strains ectopically expressing a respective CA from a replicative plasmid. We were unable to complement the ΔCA1 and ΔCA4 strains. Data in **C** represent the mean  $\pm$  SEM from two independent experiments (n = 4).

of the downstream genes resulting in the observed growth defects. Collectively, the AZM toxicity toward *M. capsulatus* and the significant growth defects of the CA knock-out strains underscore that CA activity is critical for optimal *M. capsulatus* growth.

# Carbonic anhydrase overexpression improves *M. capsulatus* growth and increases carbon conversion efficiency

The P<sub>tet</sub>-inducible CA expression plasmids developed for complementation of the KO strains were also transferred to wild-type *M. capsulatus* to analyze the effect of each isoform on *M. capsulatus* growth and C1 gas consumption/evolution. Overexpression of each isoform was confirmed *via* qRTPCR, with each isoform being induced ~10 fold over baseline when transcribed from the P<sub>tet</sub> promoter (Fig. 4A). Growth analyses of the CA overexpression strains in serum vials with CH<sub>4</sub> supplied as the only carbon source showed that increased expression of CA2 (pCA2) or CA3 (pCA3) isoforms enhanced growth compared to wild-type cultures with basal-level expression (Fig. 4B; Fig. S16). The growth enhancement of pCA2 and pCA3 was isolated to the early lag phase of growth since all CA overexpression strains had similar specific growth rates as wild-type

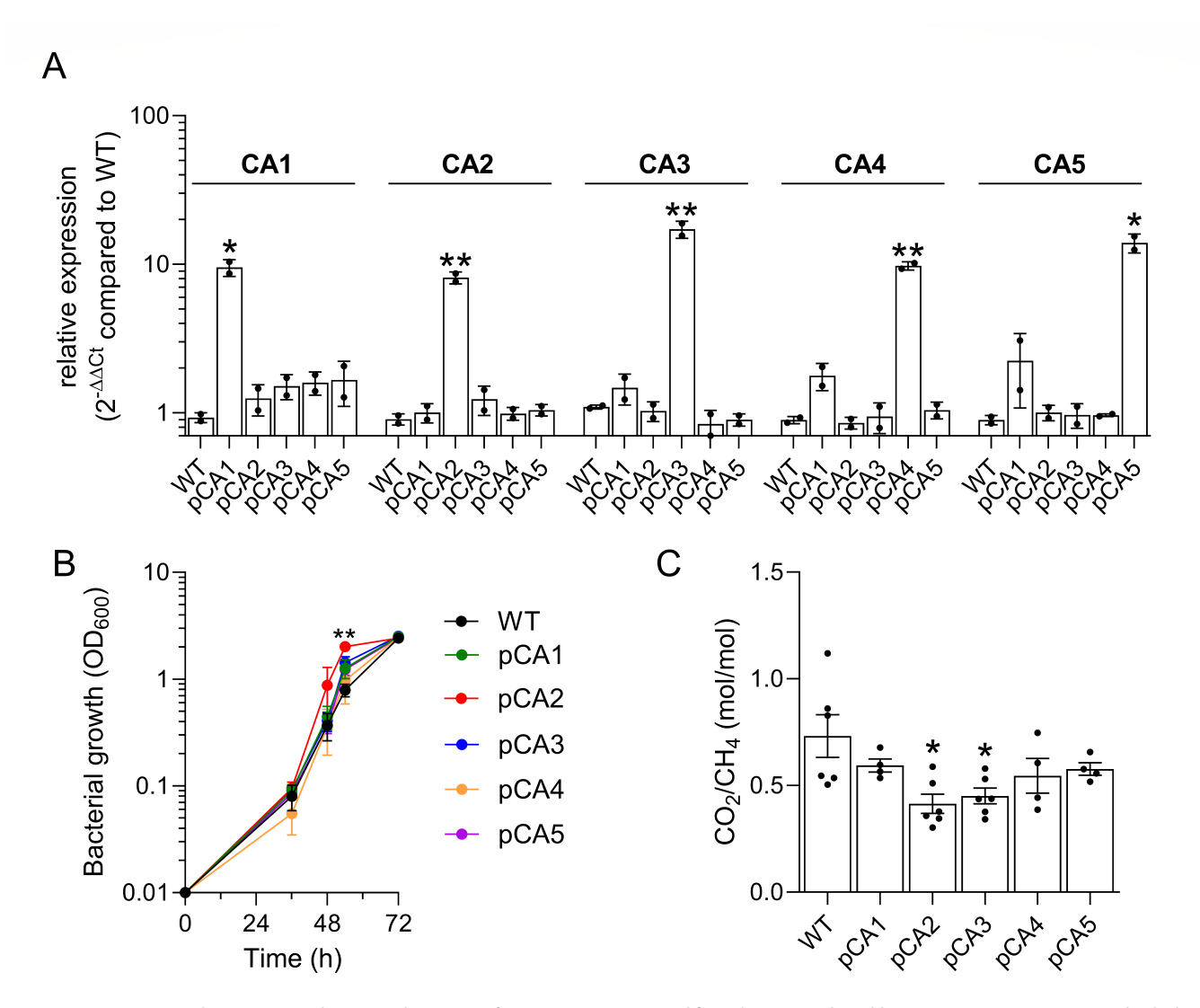


FIG 4 CA overexpression boosts *M. capsulatus* growth. (A) CA isoforms were overexpressed from the pCAH01 broad-host-range expression vector. Individual CA transcription in overexpression strains was compared to WT *via* qRT-PCR. (B) Bacterial growth of WT and CA overexpressing strains in serum vials supplied with 20% CH<sub>4</sub> in air. (C) The ratio of CO<sub>2</sub> evolved to CH<sub>4</sub> consumed by WT and CA overexpression strains to reach mid-logarithmic growth (OD<sub>600</sub> ~0.5) determined by gas chromatography. The data represent the mean  $\pm$  SD (A) or SEM (B and C) from at least two independent experiments (n = 2-6). \* $P \le 0.05$ . \* $P \le 0.01$ .

M. capsulatus, ranging from 0.094 to 0.112 h<sup>-1</sup> during logarithmic growth (Fig. S16A and B). Also, the CA overexpression strains entered the stationary phase at similar OD as wild-type M. capsulatus and accumulated comparable biomass over the duration of cultivation (Fig. 4B; Fig. S16A). Since the positive effect of CA overexpression on growth was attributed to lag phase, we evaluated gas consumption/evolution dynamics within the first 48 h of cultivation, which is the time required for cells to reach mid-logarithmic growth/metabolic steady state under our growth conditions (Table 3). M. capsulatus and the pCAx strains consumed between 106 and 133 mmol CH<sub>4</sub>/g DW with no statistical difference between the overexpression strains and wild-type cultures (Table 3; Fig. S17A). Wild-type M. capsulatus evolved 76 ± 8 mmol/g DW CO<sub>2</sub> within 48 h, which is consistent with prior gas consumption/evolution measurements reported by this methanotroph (9). However, CA overexpression strain cultures showed an 8-21 mmol CO<sub>2</sub>/g DW<sup>-1</sup> decrease in gas evolution, with pCA2 and pCA3 evolving 55  $\pm$  7 and 56  $\pm$  3 mmol CO<sub>2</sub>/g DW<sup>-1</sup>, respectively (Table 3; Fig. S17B). As such, pCA2 and pCA3 evolved less CO2 per CH4 consumed (0.41  $\pm$  0.05 and 0.45  $\pm$  0.04 mol/mol, respectively) compared to wild-type  $(0.73 \pm 0.10 \text{ mol/mol})$  (Fig. 4C; Table 3). We did not measure significant differences in biomass yield from CH<sub>4</sub> between any of the pCAx overexpression strains and wild-type M. capsulatus, indicating that the amount of formaldehyde condensation with ribulose monophosphate as part of the RuMP pathway was unaltered by CA overexpression (Table 3). However, overexpression of CA1, CA2, CA3, and CA5 variants significantly improved carbon conversion to biomass efficiency (CCE) when the CO2 evolved/CH4 consumed ratio was considered as the overall carbon assimilated to biomass (Table 3). The pCA2 and pCA3 strains showed the best overall CCE (pCA2,  $3.25 \pm 0.57$  mg DW/mol  $CO_2/mol\ CH_4$ ; pCA3, 3.09  $\pm$  0.34 mg DW/mol  $CO_2/mol\ CH_4$ ) which correlated to 2.2- and 2.1-fold improvement in biomass yield compared to wild-type (1.47  $\pm$  0.25 mg DW/mol CO<sub>2</sub>/mol CH<sub>4</sub>), respectively (Table 3), consistent with the boosted growth observed in these strains (Fig. 5A). Collectively, these results show that wild-type M. capsulatus and CA overexpression strains consumed comparable amounts of CH<sub>4</sub> and had similar biomass yield directly from CH<sub>4</sub>, but CA2 and CA3 overexpression decreased CO<sub>2</sub> accumulation in the serum vial headspace (Table 3). The decrease in CO<sub>2</sub> was not due to a decrease in complete CH<sub>4</sub> oxidation to CO<sub>2</sub> with associated higher formaldehyde flux to biomass but rather is attributed to increased CO<sub>2</sub> re-uptake, which improved biomass yield of the CA overexpression strains (Fig. 5).

We next evaluated the effect of CA2 and CA3 co-overexpression on M. capsulatus growth and gas consumption/evolution dynamics. High-resolution cell growth quantification supported that overexpression of both CA2 and CA3 improved growth compared to overexpression of either variant individually, with the pCA2-3 strain exhibiting a 14-h decreased lag phase and reaching logarithmic growth earlier than wild type (Fig. 5A). Like the individual CA overexpression strains, pCA2-3 did not accumulate more biomass/reach higher OD than wild type. The pCA2-3 strain's improved productivity was attributed to a 2.6-fold improvement in CCE (3.82  $\pm$  0.34 mg DW/mol CO<sub>2</sub>/mol CH<sub>4</sub>) over the wild type (Fig. 5B; Table 3), which was also significantly higher than the CCE improvements observed via overexpression of CA2 or CA3 individually. To further

**TABLE 3** CA overexpression strain culture metrics (48 h, logarithmic growth phase)<sup>a</sup>

Strain	CH <sub>4</sub> consumed	CO <sub>2</sub> evolved	CO <sub>2</sub> /CH <sub>4</sub>	Biomass yield	Biomass yield (mg DW/mol
	(mmol/g DW)	(mmol/g DW)	(mol/mol)	(g/g CH <sub>4</sub> )	CO <sub>2</sub> /mol CH <sub>4</sub> )
WT	114 ± 10	76 ± 8	0.73 ± 0.10	0.59 ± 0.05	1.47 ± 0.25
pCA1	$106 \pm 6$	62 ± 2	$0.59 \pm 0.03$	$0.60 \pm 0.03$	*2.85 ± 0.42
pCA2	133 ± 15	55 ± 7	**0.41 ± 0.05	$0.51 \pm 0.08$	**3.25 ± 0.57
рСА3	127 ± 6	$56 \pm 3$	**0.45 ± 0.04	$0.50 \pm 0.02$	**3.09 ± 0.34
pCA4	131 ± 14	$68 \pm 5$	$0.55 \pm 0.08$	$0.49 \pm 0.05$	1.57 ± 0.17
pCA5	112 ± 17	$64 \pm 9$	$0.58 \pm 0.03$	$0.60 \pm 0.10$	*2.64 ± 0.35
pCA2-3	$140 \pm 8$	57 ± 3	*0.41 ± 0.05	$0.45 \pm 0.03$	***3.82 ± 0.34

<sup>o</sup>Data represent the mean  $\pm$  standard error of 3–10 biological replicates from at least two independent experiments. \* $P \le 0.05$ ; \*\* $P \le 0.01$ ; \*\*\* $P \le 0.01$ ; compared to WT based on a two-tailed student's t-test.

10.1128/msphere.00496-24 **14** 

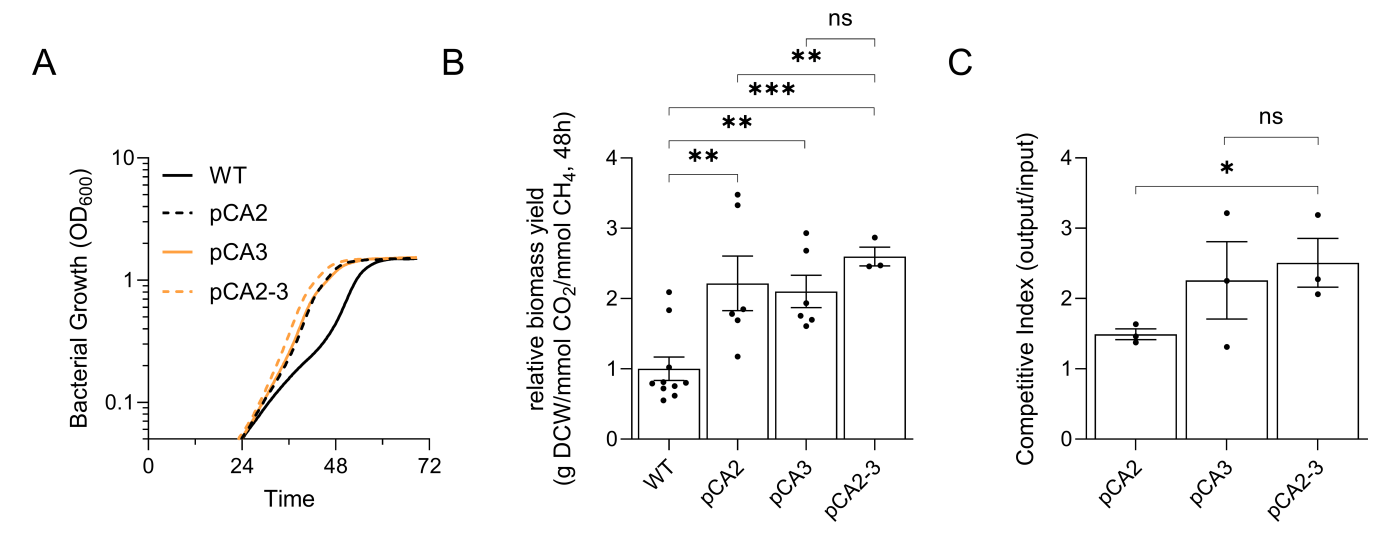


FIG 5 CA overexpression improves *Methylococcus* carbon conversion efficiency. (A) High-resolution cell growth quantification (CGQ) and (B) biomass yield calculated using the CO<sub>2</sub> evolved/CH<sub>4</sub> consumed ratio of WT and strains overexpressing CA2 (pCA2) or CA3 (pCA3) alone or in combination (pCA2-3). (C) Mixed cultures consisting of WT *M. capsulatus* and pCA2, pCA3, or pCA2-3 were cultivated for 48 h to evaluate bacterial fitness. The ratio of engineered strain (pCAx) to WT after 48 h was compared to the ratio of the inoculum by replica dilution plating on NMS solid medium with (pCAx only) or without kanamycin (WT + pCAx). The limit of detection of a CGQ sensor is OD<sub>600</sub> ~0.5, which cultures reached at ~24 h post-inoculation. The data represent the mean of two independent growth experiments (A) or the mean  $\pm$  SEM (B and C) from two independent experiments (n = 3-6). \* $P \le 0.05$ , \*\* $P \le 0.01$ , \*\*\* $P \le 0.001$ .

validate these observed CCE improvements, we performed a competition assay to compare the fitness of the pCA2, pCA3, or pCA2-3 engineered strains to wild type in a mixed culture with the hypothesis that the overexpression strains would outperform wild-type *M. capsulatus* due to increased CO<sub>2</sub> uptake. Indeed, pCA2, pCA3, and pCA2-3 outperformed wild-type 1.49-, 2.25-, and 2.51-fold, respectively (Fig. 5C), which are fitness enhancements consistent with the growth enhancements and CCE improvements measured in axenic cultures (Fig. 5B). These data highlight that CA overexpression is a viable strategy to improve CCE in a RubisCO-encoding methanotrophic biocatalyst. Furthermore, the pCA2-3 strain represents an engineered biocatalyst with enhanced biomass productivity that could improve the techno-economics of *M. capsulatus*-based single-cell protein production.

# **DISCUSSION**

Methanotrophic bacteria play vital roles in biogeochemical cycling across the globe and mitigate climate change by direct capture of the greenhouse gas CH<sub>4</sub>. *M. capsulatus* and other Type Ib Gammaproteobacterial methanotrophs encode RubisCO which mediates CO<sub>2</sub> assimilation essential for their growth, thereby limiting the overall CO<sub>2</sub> evolution from biological CH<sub>4</sub> oxidation. In this study, we have provided several lines of evidence that CAs have vital roles in the *M. capsulatus* inorganic metabolism needed for the growth of this obligate methanotroph. Our results show that increasing methanotroph CA levels improve biomass productivity while paradoxically decreasing CO<sub>2</sub> evolution, improving overall CCE to biomass. Thus, the biocatalysts with enhanced CCE and the insights developed here can be leveraged for improving CH<sub>4</sub> bioconversion processes and climate change mitigation.

*M. capsulatus* expresses five CA isoforms with phylogenetic relationships that provide insight into their possible function(s) in general methanotroph metabolism and/or the specialized dual CH<sub>4</sub> and CO<sub>2</sub> metabolism occurring in *M. capsulatus* that express RubisCO. The *M. capsulatus* β-CA1, β-CA3, β-CA4, and γ-CA5 isoforms have orthologs in Gamma- and Alphaproteobacterial methanotrophs with significant (>30%) sequence identified (Fig. S6 to S15; supplemental table files S1 and S2). The presence of these orthologs in the Gammaproteobacterial methanotroph *Methylotuvimicrobium* 

alcaliphilum 20Z that does not require  $CO_2$  for growth (18) suggests that these CAs may perform more generalized functions or have evolved unique functions in M. capsulatus. By contrast, M. capsulatus  $\alpha$ -CA2 orthologs are not common in methanotrophs but are found in an array of chemolithoautotrophic and phototrophic bacteria, highlighting a strong relationship between this CA isoform with autotrophic inorganic carbon metabolism. Many M. capsulatus  $\alpha$ -CA2 orthologs are found in facultative anaerobic phototrophs, including Rhodospirillum and Ectothiorhodospira (Fig. S7; File. S1). Notably, the M. capsulatus RubisCO large subunit's closest non-methanotroph ortholog is found in Ectothiorhodospira mobilis (92% sequence identity) (48), so perhaps several interspecies genetic exchanges have occurred between Methylococcus and chemoautotrophic bacteria, playing a part in the development of the Methylococcus dual C1 metabolism.

The five CA genes are appreciably expressed, and our data indicate that CA transcription can be induced in response to a decrease in  $CO_2$  availability (Fig. 1). Furthermore, bacterial treatment with the CA inhibitor, AZM, elicited an adaptive response resulting in an AZM-resistant phenotype that, at least partially, is attributed to CA overexpression (Fig. 2). The AZM-resistant phenotype is maintained in the absence of AZM selective pressure, pointing to genetic mutation(s) as a mechanism underlying the phenotype. AZM and other sulfonamide CA inhibitors are currently being considered as antibacterial therapeutics for the treatment of antibiotic-resistant bacterial infections (49). Our data show bacteria can develop resistance to AZM; thus, the *M. capsulatus* AZM adaptation may provide insight into pathogenic bacterial resistance strategies. Whole-genome sequencing of the AZM-resistant strains may identify mutations leading to dysregulation of CA expression or other adaptive mechanisms. For applied methanotroph biotechnologies, the identified mutations/genes would represent putative metabolic engineering targets to further improve  $CO_2$  uptake and conversion.

We hypothesized that the *M. capsulatus* cytoplasmic CAs (e.g., β-CA1, β-CA3, β-CA4, and γ-CA5) would complement the loss of other isoforms, so we were surprised to find that each CA KO strain had a substantial growth defect compared to wild-type (Fig. 3). These data highlight that each CA plays a unique, critical role in M. capsulatus metabolism and physiology, but the underlying mechanisms remain undetermined. CO2 and HCO<sub>3</sub><sup>-</sup> are required for several biochemical reactions; thus, some M. capsulatus CAs may play distinct roles in maintaining the intracellular CO<sub>2</sub>/HCO<sub>3</sub><sup>-</sup> balance for biosynthetic processes or other physiological functions rather than capturing external CO2. Each CA isoform could have unique binding partners or localization in Methylococcus, which could also explain a lack of redundancy. The M. capsulatus α-CA2 is the only secreted CA, and based on the physiological role of α-CAs in other bacteria, likely converts CO<sub>2</sub> to HCO<sub>3</sub> in the periplasmic space (28, 50). The M. capsulatus gene encoding β-CA3 is in an operon with a gene annotated to encode a SulP family inorganic anion transporter and members of this protein family have been demonstrated to transport  $HCO_3^-$  in cyanobacteria (30, 51, 52). In addition, the  $\beta$ -CA4 gene is in an operon with a downstream gene (MCA1664) annotated as a xanthine/uracil permease, which is thought to be the ancestral protein family of the SulP bicarbonate transporters (53). The M. capsulatus β-CA3 and β-CA4 genomic context implies that they may coordinate with a SulP transporter to either import or export HCO<sub>3</sub><sup>-</sup> across the periplasmic membrane. Replacement of the CA4 locus with an antibiotic resistance cassette may have negatively affected the expression of the downstream putative transporter, which may explain our inability to complement the CA4 knock-out strain.

Notably, overexpression of CA2 or CA3 significantly increased CO<sub>2</sub> assimilation compared to wild-type *M. capsulatus* (Fig. 4). The pCA2 and pCA3 strains do not have increased overall biomass accumulation compared to wild type, so the improved CCE phenotype seems to primarily be isolated to the lag phase. We speculate that after inoculation and introduction of CH<sub>4</sub> only into the serum vial headspace, *M. capsulatus* completely oxidizes a significant percentage of CH<sub>4</sub> to CO<sub>2</sub> rather than biomass until it reaches a minimum partial pressure, at which time more CH<sub>4</sub> is directed to biomass. Unfortunately, we do not yet have the resolution to define the exact CO<sub>2</sub> partial pressure

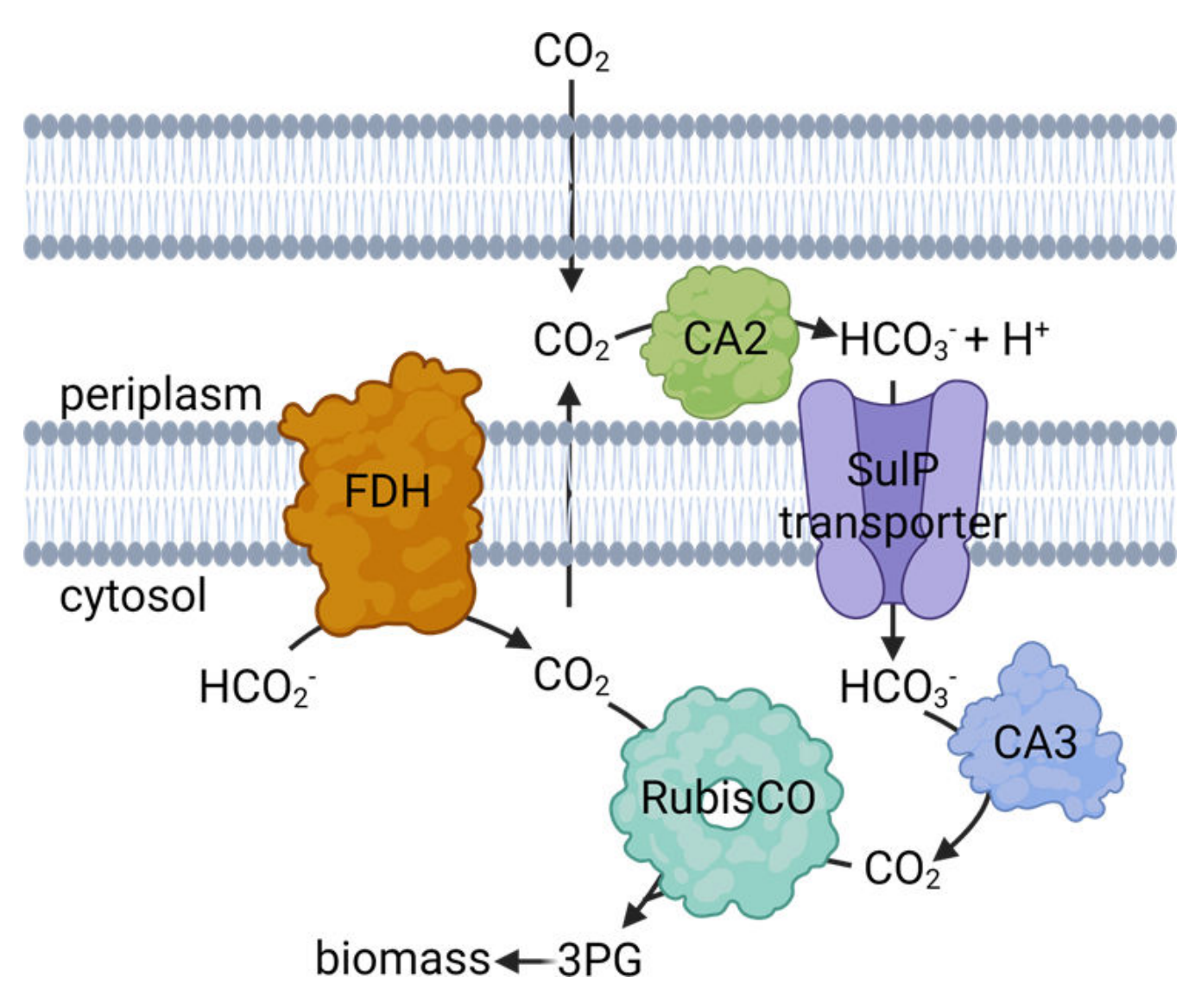


FIG 6 Working model for CO<sub>2</sub> assimilation in *M. capsulatus*. CO<sub>2</sub> is rapidly generated from the complete oxidation of CH<sub>4</sub> in methanotrophs. Under low external CO<sub>2</sub> partial pressures, CO<sub>2</sub> produced intracellularly *via* enzymatic decarboxylation reactions or formate ( $HCO_2^-$ ) dehydrogenase (FDH)-mediated oxidation of  $HCO_2^-$  can rapidly diffuse from the cell. The α-CA2 located in the periplasmic space converts CO<sub>2</sub> to  $HCO_3^-$ , which is imported by inorganic  $HCO_3^-$ /sulfate permease (SulP) family transporters. Intracellular CAs, including the β-CA3, catalyze  $HCO_3^-$  dehydration to produce CO<sub>2</sub> for assimilation by the ribulose-1,5-bisphosphate carboxylase/oxygenase (RubisCO). 3-Phosphglycerate (3 PG) generated by RubisCO enters an overlapping ribulose monophosphate/Calvin cycle to generate the C5 phosphosugars required for CH<sub>4</sub> and CO<sub>2</sub> assimilation and biomass production. Created with BioRender.com.

required for M. capsulatus to initially divide. CA overexpression may decrease the  $CO_2$  partial pressure required to initiate growth or could enable  $CO_2$  capture prior to release into the headspace. Although the mechanism is yet to be identified, CA overexpressing cultures evolve less  $CO_2$  per  $CH_4$  oxidized and the  $CO_2$  likely is converted to biomass since these strains exhibit improved productivity (i.e., faster biomass accumulation). We observed an additive growth enhancement with improved  $CO_2$  assimilation when the  $\alpha$ -CA2 and  $\beta$ -CA3 were co-overexpressed (Fig. 4 and 5). Given that the  $\beta$ -CA3 is co-expressed with a bicarbonate transporter and the  $\alpha$ -CA2 is secreted, these data lead us to a model wherein the  $\alpha$ -CA2 converts  $CO_2$  to bicarbonate in the periplasm, which is imported across the periplasmic membrane by the SuIP family transporter and converted to  $CO_2$  in the cytoplasm by the  $\beta$ -CA3, increasing RubisCO substrate availability (Fig. 6). This speculative carbon concentration mechanism needs to be experimentally tested but is a possible explanation for the phenotypes observed here.

Technoeconomic analyses have identified CCE and productivity as primary cost drivers in CH<sub>4</sub> bioconversion processes using methanotrophic bacteria (54). A twofold improvement in CCE in natural gas to lactate conversion bioprocess can decrease the lactate minimal selling price (\$/kg) by 34%, which is primarily due to an overall decrease in capital expenditures (54). The engineered strain developed here (pCA2-3) has a 2.5-fold increase in CCE (Fig. 5). As such, using this strain to convert CH<sub>4</sub>-rich natural gas or anaerobic digestion-derived biogas to valuable products (e.g., lactate) or microbial biomass/single-cell protein would immediately reduce production costs. Further strain improvements to enhance CO<sub>2</sub> assimilation/CCE, increase product titer and productivity, and bioprocess optimization could lead to dramatic cost reductions to facilitate the commercialization of CH<sub>4</sub> bioconversion processes.

Methanotroph-dependent conversion of CH<sub>4</sub> represents an approach to capture GHGs and mitigate climate change. Here, we have advanced our understanding of the dual CH<sub>4</sub> and CO<sub>2</sub> metabolism occurring in the methanotroph, *Methylococcus capsulatus*, a methanotroph currently used industrially to produce single-cell protein. These and future insights into the *M. capsulatus* metabolism and physiology will guide strain improvement strategies required to realize the effective use of these biocatalysts in biotechnology applications.

#### **ACKNOWLEDGMENTS**

We thank Dr. Sami Ben Said, Sreemoye Nath, and Selina Aguilar for their technical assistance. This work was funded by University of North Texas start-up funds and National Science Foundation MCB award #2225776 to CH.

S.L., J.H., R.A., C.B., and T.M. developed bacterial strains and performed experiments; S.L. and C.H. conceptualized the research. C.H. acquired funding and supervised the research. S.L. and C.H. wrote the paper with input from all authors.

### **AUTHOR AFFILIATION**

<sup>1</sup>BioDiscovery Institute and Department of Biological Sciences, University of North Texas, Denton, Texas, USA

### **AUTHOR ORCIDs**

Calvin A. Henard http://orcid.org/0000-0002-4574-587X

# **FUNDING**

Funder	Grant(s)	Author(s)
National Science Foundation (NSF)	MCB#22257760	Calvin A. Henard

### **AUTHOR CONTRIBUTIONS**

Spencer A. Lee, Formal analysis, Investigation, Writing – original draft, Writing – review and editing | Jessica M. Henard, Investigation, Writing – review and editing | Robyn A. C. Alba, Investigation, Writing – review and editing | Chance A. Benedict, Investigation, Writing – review and editing | Tyler A. Mayes, Investigation, Writing – review and editing | Calvin A. Henard, Conceptualization, Formal analysis, Funding acquisition, Project administration, Resources, Supervision, Writing – original draft, Writing – review and editing

### **ADDITIONAL FILES**

The following material is available online.

### Supplemental Material

Supplemental figures (mSphere00496-24-s0001.pdf). Figures S1 to S17.

Tables S1 to S5 (mSphere00496-24-s0002.xlsx). Blastp results tables.

Tables S6 to S10 (mSphere00496-24-s0003.xlsx). Blastp methanotroph results tables.

#### **REFERENCES**

- Rao CV, Mackie RI, Parker DA, Shears JH. 2023. Biological methane conversion, p 199–226. In Galvita V, Bos R (ed), Methane conversion routes: status and prospects. Royal Society of Chemistry.
- Kang NK, Chau THT, Lee EY. 2024. Engineered methane biocatalysis: strategies to assimilate methane for chemical production. Curr Opin Biotechnol 85:103031. https://doi.org/10.1016/j.copbio.2023.103031
- Lidstrom ME. 2024. Direct methane removal from air by aerobic methanotrophs. Cold Spring Harb Perspect Biol 16:a041671. https://doi. org/10.1101/cshperspect.a041671
- He L, Groom JD, Wilson EH, Fernandez J, Konopka MC, Beck DAC, Lidstrom ME. 2023. A methanotrophic bacterium to enable methane removal for climate mitigation. Proc Natl Acad Sci U S A 120:e2310046120. https://doi.org/10.1073/pnas.2310046120
- Sakai Y, Yurimoto H, Shima S. 2023. Methane monooxygenases; physiology, biochemistry and structure. Catal Sci Technol 13:6342–6354. https://doi.org/10.1039/D3CY00737E
- Tucci FJ, Rosenzweig AC. 2024. Direct methane oxidation by copper- and iron-dependent methane monooxygenases. Chem Rev 124:1288–1320. https://doi.org/10.1021/acs.chemrev.3c00727
- Kalyuzhnaya MG, Gomez OA, Murrell JC. 2019. The methane-oxidizing bacteria (methanotrophs), p 1–34. In McGenity TJ (ed), Taxonomy, genomics and ecophysiology of hydrocarbon-degrading microbes. Springer International Publishing, Cham.
- 8. Dedysh SN, Knief C. 2018. Diversity and phylogeny of described aerobic methanotrophs, p 17–42. In Kalyuzhnaya MG, Xing XH (ed), Methane biocatalysis: paving the way to sustainability. Springer International Publishing, Cham.
- Leak DJ, Dalton H. 1986. Growth yields of methanotrophs. Appl Microbiol Biotechnol 23:470–476. https://doi.org/10.1007/BF02346062
- Park S, Hanna L, Taylor RT, Droege MW. 1991. Batch cultivation of Methylosinus trichosporium OB3b. I: production of soluble methane monooxygenase. Biotechnol Bioeng 38:423–433. https://doi.org/10. 1002/bit.260380412
- Khadem AF, Pol A, Wieczorek A, Mohammadi SS, Francoijs K-J, Stunnenberg HG, Jetten MSM, Op den Camp HJM. 2011. Autotrophic methanotrophy in verrucomicrobia: Methylacidiphilum fumariolicum SolV uses the Calvin-Benson-Bassham cycle for carbon dioxide fixation. J Bacteriol 193:4438–4446. https://doi.org/10.1128/JB.00407-11
- Ward N, Larsen Ø, Sakwa J, Bruseth L, Khouri H, Durkin AS, Dimitrov G, Jiang L, Scanlan D, Kang KH, et al. 2004. Genomic insights into methanotrophy: the complete genome sequence of *Methylococcus capsulatus* (Bath). PLoS Biol 2:e303. https://doi.org/10.1371/journal.pbio. 0020303
- Balasubramanian R, Smith SM, Rawat S, Yatsunyk LA, Stemmler TL, Rosenzweig AC. 2010. Oxidation of methane by a biological dicopper centre. Nature 465:115–119. https://doi.org/10.1038/nature08992
- Koo CW, Tucci FJ, He Y, Rosenzweig AC. 2022. Recovery of particulate methane monooxygenase structure and activity in a lipid bilayer. Science 375:1287–1291. https://doi.org/10.1126/science.abm3282
- Csáki R, Bodrossy L, Klem J, Murrell JC, Kovács KL. 2003. Genes involved in the copper-dependent regulation of soluble methane monooxygenase of Methylococcus capsulatus (Bath): cloning, sequencing and mutational analysis. Microbiology (Reading) 149:1785–1795. https://doi. org/10.1099/mic.0.26061-0
- Larsen Ø, Karlsen OA. 2016. Transcriptomic profiling of Methylococcus capsulatus (Bath) during growth with two different methane monooxygenases. Microbiologyopen 5:254–267. https://doi.org/10.1002/mbo3. 324
- Orata FD, Meier-Kolthoff JP, Sauvageau D, Stein LY. 2018. Phylogenomic analysis of the gammaproteobacterial methanotrophs (order Methylococcales) calls for the reclassification of members at the genus

- and species levels. Front Microbiol 9:3162. https://doi.org/10.3389/fmicb.2018.03162
- Henard CA, Wu C, Xiong W, Henard JM, Davidheiser-Kroll B, Orata FD, Guarnieri MT. 2021. Ribulose-1,5-bisphosphate carboxylase/oxygenase (RubisCO) is essential for growth of the methanotroph *Methylococcus capsulatus* strain bath. Appl Environ Microbiol 87:e0088121. https://doi. org/10.1128/AEM.00881-21
- Baxter NJ, Hirt RP, Bodrossy L, Kovacs KL, Embley TM, Prosser JI, Murrell JC. 2002. The ribulose-1,5-bisphosphate carboxylase/oxygenase gene cluster of *Methylococcus capsulatus* (Bath). Arch Microbiol 177:279–289. https://doi.org/10.1007/s00203-001-0387-x
- Stanley SH, Dalton H. 1982. Role of ribulose-1,5-bisphosphate carboxylase/oxygenase in *Methylococcus capsulatus* (Bath). Microbiology 128:2927–2935. https://doi.org/10.1099/00221287-128-12-2927
- Taylor SC, Dalton H, Dow CS. 1981. Ribulose-1,5-bisphosphate carboxylase/oxygenase and carbon assimilation in *Methylococcus* capsulatus (Bath). Microbiology 122:89–94. https://doi.org/10.1099/ 00221287-122-1-89
- Erb TJ, Zarzycki J. 2018. A short history of RubisCO: the rise and fall (?) of Nature's predominant CO<sub>2</sub> fixing enzyme. Curr Opin Biotechnol 49:100– 107. https://doi.org/10.1016/j.copbio.2017.07.017
- Appel AM, Bercaw JE, Bocarsly AB, Dobbek H, DuBois DL, Dupuis M, Ferry JG, Fujita E, Hille R, Kenis PJA, Kerfeld CA, Morris RH, Peden CHF, Portis AR, Ragsdale SW, Rauchfuss TB, Reek JNH, Seefeldt LC, Thauer RK, Waldrop GL. 2013. Frontiers, opportunities, and challenges in biochemical and chemical catalysis of CO<sub>2</sub> fixation. Chem Rev 113:6621–6658. https://doi.org/10.1021/cr300463y
- Kerfeld CA, Aussignargues C, Zarzycki J, Cai F, Sutter M. 2018. Bacterial microcompartments. Nat Rev Microbiol 16:277–290. https://doi.org/10. 1038/nrmicro.2018.10
- Supuran CT, Capasso C. 2017. An overview of the bacterial carbonic anhydrases. Metabolites 7:56. https://doi.org/10.3390/metabo7040056
- DiMario RJ, Machingura MC, Waldrop GL, Moroney JV. 2018. The many types of carbonic anhydrases in photosynthetic organisms. Plant Sci 268:11–17. https://doi.org/10.1016/j.plantsci.2017.12.002
- Smith KS, Ferry JG. 2000. Prokaryotic carbonic anhydrases. FEMS Microbiol Rev 24:335–366. https://doi.org/10.1111/j.1574-6976.2000. tb00546.x
- Gai CS, Lu J, Brigham CJ, Bernardi AC, Sinskey AJ. 2014. Insights into bacterial CO<sub>2</sub> metabolism revealed by the characterization of four carbonic anhydrases in *Ralstonia eutropha* H16. AMB Express 4:2. https:// doi.org/10.1186/2191-0855-4-2
- Kerfeld CA, Melnicki MR. 2016. Assembly, function and evolution of cyanobacterial carboxysomes. Curr Opin Plant Biol 31:66–75. https://doi. org/10.1016/j.pbi.2016.03.009
- Felce J, Saier MH. 2004. Carbonic anhydrases fused to anion transporters of the SulP family: evidence for a novel type of bicarbonate transporter. J Mol Microbiol Biotechnol 8:169–176. https://doi.org/10.1159/000085789
- Jo BH, Kim IG, Seo JH, Kang DG, Cha HJ. 2013. Engineered Escherichia coli with periplasmic carbonic anhydrase as a biocatalyst for CO<sub>2</sub> sequestration. Appl Environ Microbiol 79:6697–6705. https://doi.org/10.1128/ AEM.02400-13
- Tu W, Xu J, Thompson IP, Huang WE. 2023. Engineering artificial photosynthesis based on rhodopsin for CO<sub>2</sub> fixation. Nat Commun 14:8012. https://doi.org/10.1038/s41467-023-43524-4
- Bhagat C, Dudhagara P, Tank S. 2018. Trends, application and future prospectives of microbial carbonic anhydrase mediated carbonation process for CCUS. J Appl Microbiol 124:316–335. https://doi.org/10. 1111/jam.13589
- Bose H, Satyanarayana T. 2017. Microbial carbonic anhydrases in biomimetic carbon sequestration for mitigating global warming:

10.1128/msphere.00496-24 **19** 

- prospects and perspectives. Front Microbiol 8:1615. https://doi.org/10. 3389/fmicb.2017.01615
- 35. Yong JKJ, Stevens GW, Caruso F, Kentish SE. 2015. The use of carbonic anhydrase to accelerate carbon dioxide capture processes. J Chem Technol Biotechnol 90:3–10. https://doi.org/10.1002/jctb.4502
- Alvizo O, Nguyen LJ, Savile CK, Bresson JA, Lakhapatri SL, Solis EOP, Fox RJ, Broering JM, Benoit MR, Zimmerman SA, Novick SJ, Liang J, Lalonde JJ. 2014. Directed evolution of an ultrastable carbonic anhydrase for highly efficient carbon capture from flue gas. Proc Natl Acad Sci U S A 111:16436–16441. https://doi.org/10.1073/pnas.1411461111
- Tapscott T, Guarnieri MT, Henard CA. 2019. Development of a CRISPR/ Cas9 system for Methylococcus capsulatus in vivo gene editing. Appl Environ Microbiol 85:e00340-19. https://doi.org/10.1128/AEM.00340-19
- Henard CA, Smith H, Dowe N, Kalyuzhnaya MG, Pienkos PT, Guarnieri MT. 2016. Bioconversion of methane to lactate by an obligate methanotrophic bacterium. Sci Rep 6:21585. https://doi.org/10.1038/ srep21585
- Schäfer A, Tauch A, Jäger W, Kalinowski J, Thierbach G, Pühler A. 1994.
   Small mobilizable multi-purpose cloning vectors derived from the Escherichia coli plasmids pK18 and pK19: selection of defined deletions in the chromosome of Corynebacterium glutamicum. Gene 145:69–73. https://doi.org/10.1016/0378-1119(94)90324-7
- Hoang TT, Karkhoff-Schweizer RR, Kutchma AJ, Schweizer HP. 1998. A broad-host-range Flp-FRT recombination system for site-specific excision of chromosomally-located DNA sequences: application for isolation of unmarked *Pseudomonas aeruginosa* mutants. Gene 212:77– 86. https://doi.org/10.1016/s0378-1119(98)00130-9
- Datsenko KA, Wanner BL. 2000. One-step inactivation of chromosomal genes in *Escherichia coli* K-12 using PCR products. Proc Natl Acad Sci U S A 97:6640–6645. https://doi.org/10.1073/pnas.120163297
- Nath S, Henard JM, Henard CA. 2022. Optimized tools and methods for methanotroph genome editing. Methods Mol Biol 2489:421–434. https://doi.org/10.1007/978-1-0716-2273-5\_21
- Ishikawa M, Yokoe S, Kato S, Hori K. 2018. Efficient counterselection for Methylococcus capsulatus (Bath) by using a mutated pheS gene. Appl Environ Microbiol 84:e01875-18. https://doi.org/10.1128/AEM.01875-18
- Mitsuhashi S, Mizushima T, Yamashita E, Yamamoto M, Kumasaka T, Moriyama H, Ueki T, Miyachi S, Tsukihara T. 2000. X-ray structure of betacarbonic anhydrase from the red alga, *Porphyridium purpureum*, reveals a novel catalytic site for CO(2) hydration. J Biol Chem 275:5521–5526. https://doi.org/10.1074/jbc.275.8.5521

- 45. Kisker C, Schindelin H, Alber BE, Ferry JG, Rees DC. 1996. A left-hand beta-helix revealed by the crystal structure of a carbonic anhydrase from the archaeon *Methanosarcina thermophila*. EMBO J 15:2323–2330.
- Mallis RJ, Poland BW, Chatterjee TK, Fisher RA, Darmawan S, Honzatko RB, Thomas JA. 2000. Crystal structure of S-glutathiolated carbonic anhydrase III. FEBS Lett 482:237–241. https://doi.org/10.1016/s0014-5793(00)02022-6
- Teufel F, Almagro Armenteros JJ, Johansen AR, Gíslason MH, Pihl SI, Tsirigos KD, Winther O, Brunak S, von Heijne G, Nielsen H. 2022. SignalP 6.0 predicts all five types of signal peptides using protein language models. Nat Biotechnol 40:1023–1025. https://doi.org/10.1038/s41587-021-01156-3
- Tourova TP, Spiridonova EM, Berg IA, Kuznetsov BB, Sorokin DY. 2005. Phylogeny of ribulose-1,5-bisphosphate carboxylase/oxygenase genes in haloalkaliphilic obligately autotrophic sulfur-oxidizing bacteria of the genus *Thioalkalivibrio*. Microbiology 74:321–328. https://doi.org/10. 1007/s11021-005-0070-3
- Nocentini A, Capasso C, Supuran CT. 2023. Carbonic anhydrase inhibitors as novel antibacterials in the era of antibiotic resistance: where are we now? Antibiotics (Basel) 12:142. https://doi.org/10.3390/ antibiotics12010142
- Dobrinski KP, Boller AJ, Scott KM. 2010. Expression and function of four carbonic anhydrase homologs in the deep-sea chemolithoautotroph *Thiomicrospira crunogena*. Appl Environ Microbiol 76:3561–3567. https:// doi.org/10.1128/AEM.00064-10
- Price GD, Woodger FJ, Badger MR, Howitt SM, Tucker L. 2004. Identification of a SulP-type bicarbonate transporter in marine cyanobacteria. Proc Natl Acad Sci U S A 101:18228–18233. https://doi.org/10.1073/pnas. 0405211101
- Shelden MC, Howitt SM, Price GD. 2010. Membrane topology of the cyanobacterial bicarbonate transporter, BicA, a member of the SulP (SLC26A) family. Mol Membr Biol 27:12–22. https://doi.org/10.3109/ 09687680903400120
- Nayak N, Mehrotra R, Mehrotra S. 2023. BicA and related proteins of the SulP family diverged from a common ancestor with archaeal NCS-2 proteins. Res Sq. https://doi.org/10.21203/rs.3.rs-2623005/v1
- Fei Q, Liang B, Tao L, Tan ECD, Gonzalez R, Henard CA, Guarnieri MT.
   2020. Biological valorization of natural gas for the production of lactic acid: techno-economic analysis and life cycle assessment. Biochem Eng J 158:107500. https://doi.org/10.1016/j.bej.2020.107500